

# Review of Fatigue Assessment Approaches for Welded Marine Joints and Structures

Pasqualino Corigliano \* and Vincenzo Crupi

Department of Engineering, University of Messina, 98166 Messina, Italy; crupi.vincenzo@unime.it

\* Correspondence: pcorigliano@unime.it

**Abstract:** Welded joints are widely used in many sectors and represent the main joining technique also in the marine industry. The welded joints are sites of high stress concentrations and are subject to severe conditions for the marine environment. The design of marine welded joints has to consider the effects from wave loads, ship motions and loading/unloading operations and corrosion effects. The aim of this scientific work is to discuss about the state of the art of the standards and the approaches for predicting the fatigue life of welded joints used for the marine industry. Several approaches are examined in order to provide an overview and highlight the advantages and limitations of each method. Furthermore, recent advances in welding of dissimilar metals and autonomous welding are considered.

**Keywords:** welded joints; marine structures; fatigue life; local approaches

**Citation:** Corigliano, P.; Crupi, V. Review of Fatigue Assessment Approaches for Welded Marine Joints and Structures. *Metals* **2022**, *12*, 1010. <https://doi.org/10.3390/met12061010>

Academic Editor: António Bastos Pereira

Received: 15 May 2022

Accepted: 11 June 2022

Published: 14 June 2022

**Publisher's Note:** MDPI stays neutral with regard to jurisdictional claims in published maps and institutional affiliations.



**Copyright:** © 2022 by the authors. Licensee MDPI, Basel, Switzerland. This article is an open access article distributed under the terms and conditions of the Creative Commons Attribution (CC BY) license (<https://creativecommons.org/licenses/by/4.0/>).

## 1. Introduction

Fatigue is one of the most significant failure modes for ship and offshore structures [1]. The ship structures are exposed to harsh environmental cyclic loading from wave pressure, ship motions and loading/unloading procedures that cause fatigue failure [1,2]. The fractures in ship structures are frequently due to fatigue (Figure 1).

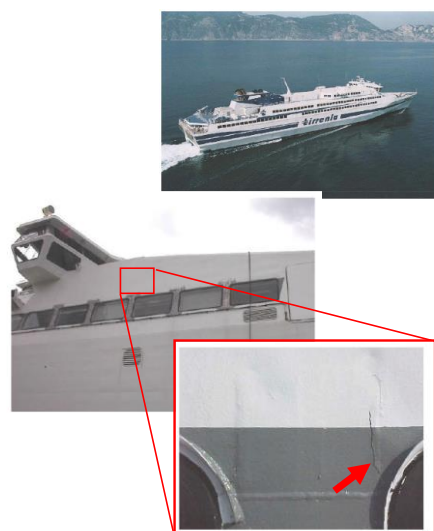


**Figure 1.** Fatigue cracks in ship structures.

Ship structures are mainly made of longitudinal and transverse details connected by welded joints. Figure 2 illustrates some typical applications of weld types in shipbuilding and the related welding processes. The welding processes, which are most commonly used in shipbuilding, are flux-cored arc welding (FCAWs), submerged arc welding

(SAW), Gas Metal Arc Welding (GMAW), Electro gas arc welding (EGW), Hybrid laser-arc welding (HLAW), double sided and one sided, automatic, portable welder, line welder, semiautomatic, and robotic.

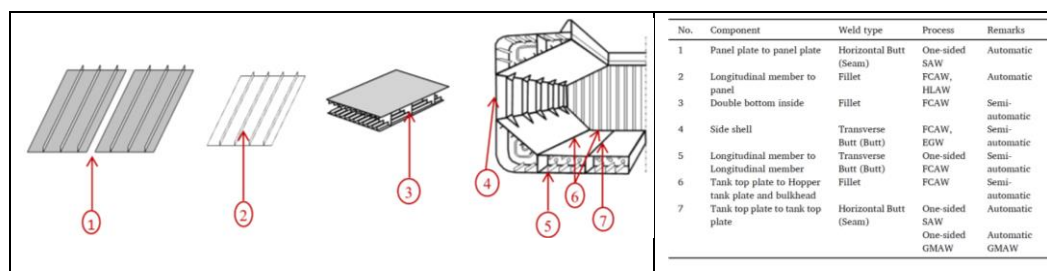


**Figure 2.** Typical weld types and processes in shipbuilding. Reprinted with permission from ref. [1]. Copyright 2021 Elsevier.

The welds are generally a weak point of the structure, due to the presence of possible crack-like defects along with high stress concentration effects and tensile residual stresses caused by the thermal welding process itself, so a fatigue design is required (Figure 3) for the fatigue life prediction of ship welded details [2–4].

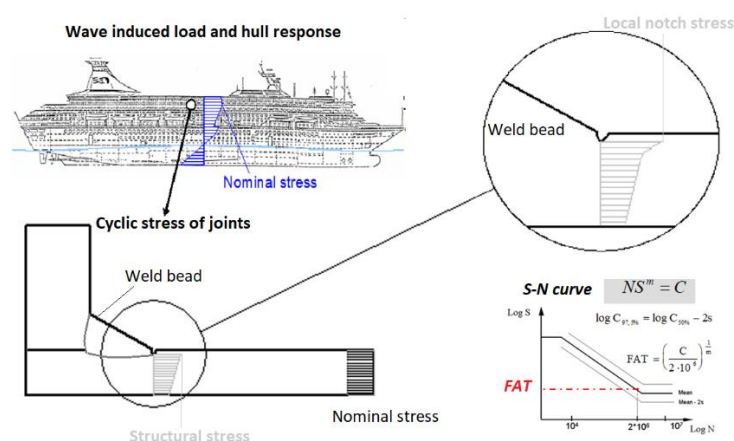


**Figure 3.** Fatigue design of ship welded structures.

The offshore infrastructure has extended its application from the oil and gas industry to the emerging offshore wind industry. The offshore structures [1,5–7] and oil and gas pipelines [8] are subjected to fatigue loadings, and fatigue cracks can be detected. Figure 4 shows the crack at the weld seam of an offshore platform [9].



**Figure 4.** Crack at weld seam of offshore platform [9].

The offshore structures are mainly composed of steel tubular members with circular hollow sections, which are interconnected by welded joints. This connection is referred to as the tubular joint. If the tubular joint consists of two pipes with different diameters, the larger diameter pipe is called the chord, and the smaller one is known as the brace. Figure 5 shows tubular joints, which are most commonly used in offshore structures.

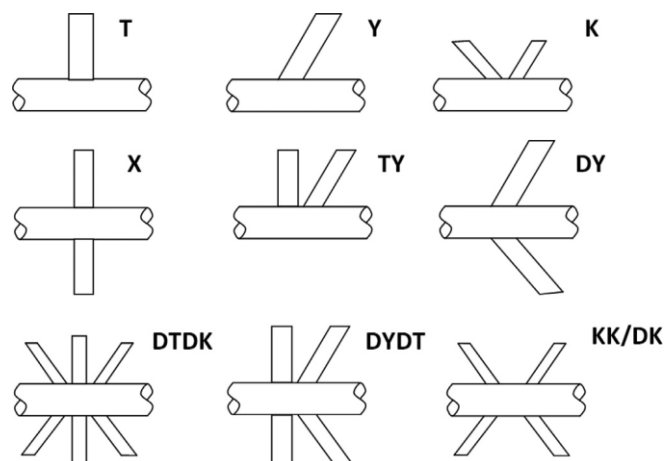


**Figure 5.** Types of tubular joints along with their nomenclature [10].

A review of corrosion fatigue in offshore structures is reported in [11], and its results show that the corrosion fatigue crack growth behavior of steel welded joints in marine environments depends on several parameters (material, environment, loading conditions, microstructure, welding procedure and residual stresses).

Static and fatigue tests were recently performed on a large-scale detail of hybrid tubular joints (Figure 6) for an offshore wind turbine in [12]. The tests demonstrated that these kinds of hybrid joints, made by combining adhesives together with welding, can be successfully used in offshore structures, as the fatigue strength is improved.

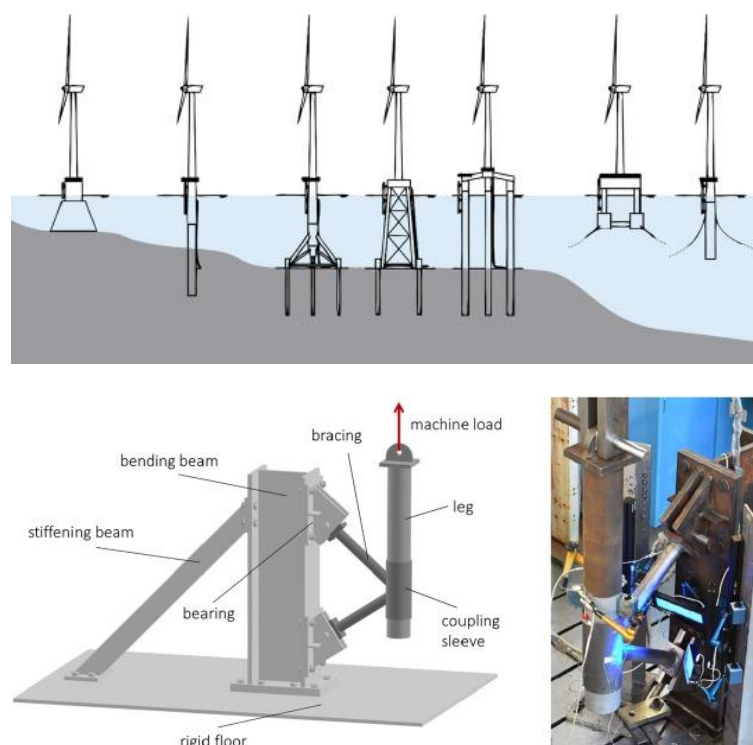


**Figure 6.** Large-scale detail of hybrid tubular joints for offshore wind turbine investigated in [12]. Reprinted with permission from ref. [12]. Copyright 2022 Elsevier.

The fatigue strength and durability of welded structures are strongly related to several parameters: the local geometrical discontinuity (weld toe radius, flank angle and weld size), the service loadings, the environmental conditions, the thickness plate, the manufacturing process, the residual stresses initiated during the welding process, the defects, and the material properties. Thus, this produces a great scatter in the fatigue life of the welded joints.

The local mechanical properties are expected to change from the weld metal (WM) to the heat-affected zone (HAZ), and generally they will be different from the base material (BM). In a previous study of the authors [13], they developed a new procedure, which is based on the following steps: the hardness measurements using the UCI (ultrasonic contact impedance) method for the identification of the different zones (BM, HAZ, and WM), the assessment of their cyclic stress–strain curves depending on the hardness values, and the realization of a nonlinear FEA, considering the different material properties. Figure 7 shows the different material zones derived from the UCI method.

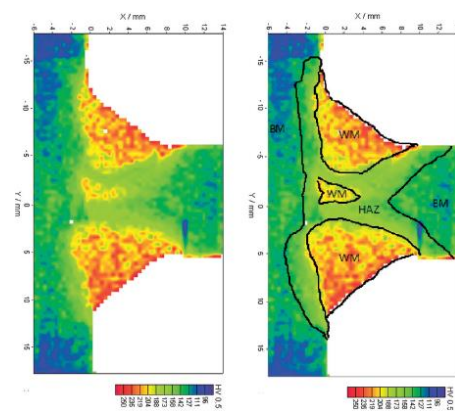


**Figure 7.** Hardness measurement results and identification of the three zones (WM, HAZ, BM) [13].

Nowadays, the shipbuilding industry is engaged in the construction of ships with structures significantly thinner than those of the traditional ships. Thus, the influence of the plate thickness on the fatigue response of the welded joint is an important parameter. It is well known that there is a reduction in the fatigue strength when the size of the structural element increases. This is due mainly to the presence of higher tensile residual stresses in the way of welds and to higher notch stresses caused by the through-thickness stress gradient that arise at geometrical discontinuities. The thickness effect is mainly explained by the geometrical size effect, shown in Figure 8: when a crack with the same length is considered for two welded joints with different thicknesses and subjected to the same nominal stress, the local stress at the tip turns out to be lower in the thinner joint as a consequence of its steeper stress gradient [14].

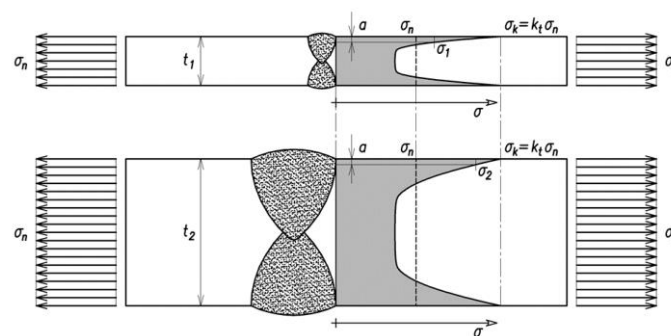


**Figure 8.** Through-thickness stress gradient in the welded joint [15].

Moreover, the thickness effect is also due to the increment of the probability of defects when the size of the structural element increases.

Ship hull and offshore structures, generally, consist of steel components connected by welded joints and, unfortunately, the formation of defects is inherent to the welding technology. These defects can grow into propagating fatigue cracks under repeated application of the dynamic loads during the service life.

The weld imperfections can be classified into three categories: planar flaws (cracks, lack of fusion or penetration, undercut and overlap), non-planar flaws (cavities and solid inclusions), and geometrical imperfections (axial misalignment, angular misalignment, imperfect weld profile, and shape imperfection). A defect is an unacceptable flaw. Figure 9 illustrates the types of common weld defects.

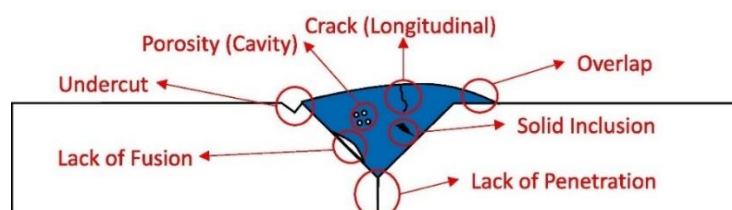


**Figure 9.** Common weld defects [3]. Reprinted with permission from ref. [3]. Copyright 2021 Elsevier.

The fatigue strength of the welded joints is, generally, lower than that of the notched components and base material as shown in Figure 10a. The size and location of the weld defects significantly affect the fatigue life of the welded joints, as supported by the Kitagawa diagram in Figure 10b.

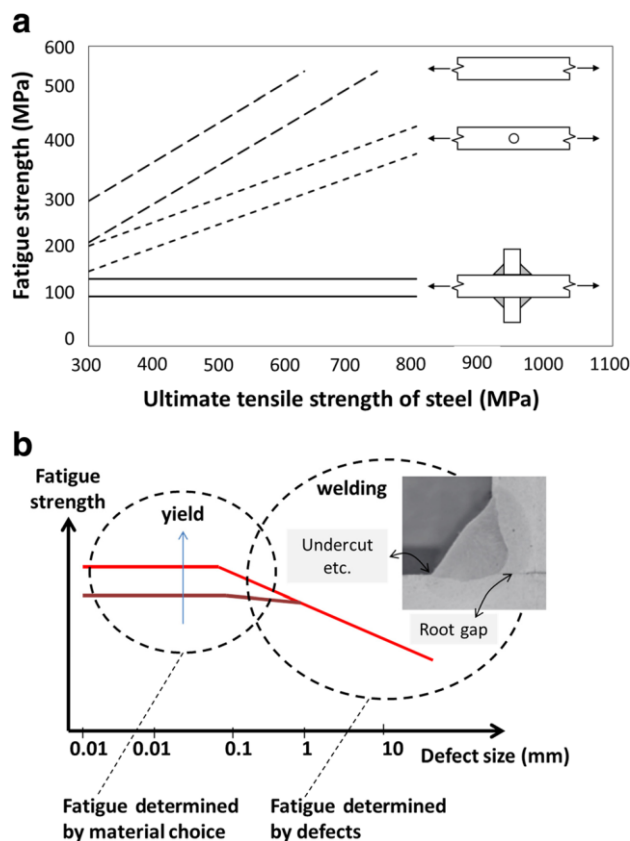


**Figure 10.** (a) Schematic illustration of fatigue strength in base material and notched and welded components. (b) Kitagawa diagram, fatigue strength versus defect size, with indicated weld positions [16].



Since defects are common in welds, the current international standard and Classification Societies should take into account the weld quality, which is defined, as reported in [16], as “the weld quality quantifies the welded joints’ ability to perform the functional requirements of the weld during the service life of the structure”, so the required level of weld quality depends on the application according to the concept of “design for purpose” [16]. The “IIW guidelines on weld quality in relationship to fatigue strength” [17] was recently published by the Institute of Welding (IIW). The weld quality should be assured at a shipyard through appropriate non-destructive testing (NDT) methods. NDT methods, used in shipbuilding, can be classified into surface testing (visual testing (VT), magnetic particle testing (MPT), and dye penetrant testing (DPT)) and volumetric testing (ultrasonic testing (UT), and radiography testing (RT)). UT is more efficient in detecting planar defects, which are more dangerous for fatigue. For thickness below 8 mm, UT cannot be used, so RT, able to detect nonplanar defects, should be used in conjunction with MPT or DPT. The weld defect length data, mainly collected by RT from the inspection of two ships, were investigated and analyzed in [3]. An overview of weld quality control and assurance of welded structures subjected to fatigue loading was provided by Stenberg et al. [16]

The ships can contain hundreds of kilometers of weld lines, so only a limited number of welded joints can be inspected, and the Classification Societies specify a number of checkpoints for the inspection. Thus, a risk-based inspection approach could be applied [18]. Figure 11 shows a typical NDT inspection plan of a ship with the checkpoints highlighted in green.

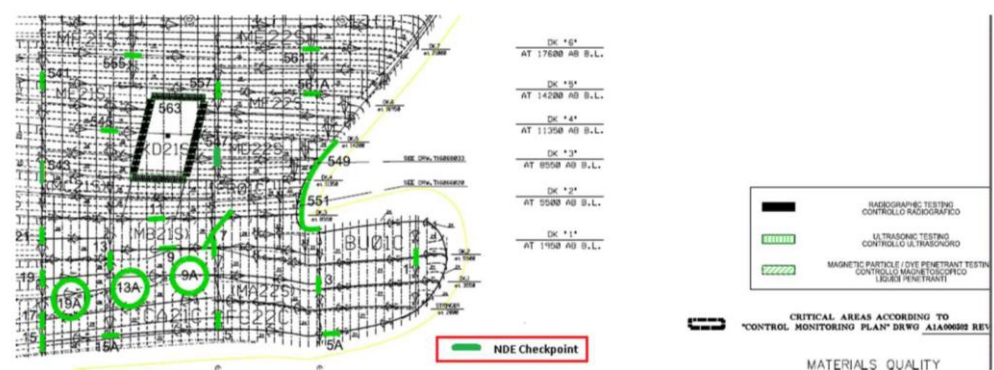


**Figure 11.** A typical NDT inspection plan [18].

Some fatigue cracks have been detected in the ship structures within a few years of their service life. The occurrence of one or more welds, which are spots of high stress concentrations, together with fatigue loads, induce local cyclic stresses that can go over the yielding stress. The fatigue cracks, which result from the presence of high stress concentrations, are related to low cycle fatigue (LCF), but existing design codes do not properly consider LCF problems. A review of experimental studies for a LCF test of a welded joint specimen was presented by Madi et al. [19]. Thus, besides high-cycle fatigue (HCF), marine structures suffer also from LCF loadings caused by the operational and the environmental conditions.

Marine structures are exposed to severe seas and long-term wave loads. Wave induced stresses are one of the main sources of fatigue damage, thus it is important to consider and simulate the wave-induced loadings and stresses. Wave-produced fluctuating stresses are stochastic in the short term and regularly spread in the long term. A procedure of creating the fatigue loading spectrum for complex marine structures centered on a design wave approach was proposed in [20]. The generated random sea states effect, according to the Pierson–Moskowitz model, on the fatigue of explosive welded Al/Fe transition joints, made with four layers of aluminum alloy A5083, A1050, Titanium Grade 1 and steel Grade D, was investigated in [21]. The fatigue life was estimated by means of the

frequency domain method, and the probability density functions were assessed applying traditional formula. The predicted results were compared with the standard test results, confirming that the predicted values did not overestimate the fatigue life.

The stochastic characteristics of the hull vibration superimposed stress waveform experienced by 6500 TEU container ship's deck longitudinal were analyzed in [22]. The authors developed an electric exciter-driven plate bending vibration fatigue testing machine, which is able to carry out the whipping superimposed fatigue tests of welded joints, and it was found that rainflow counting produces conservative estimates of the fatigue lives.

The marine aggressive environment on ship and offshore structures accelerates fatigue damage through corrosion, which causes a deterioration of the mechanical properties [23] and lowers the fatigue strength of marine welded structures. Garbatov et al. [24] considered the fatigue strength of corroded specimens of a transverse stiffened welded plate, showing the results of lower fatigue strength than expected.

The recent increase in Arctic shipping and operations requires a specific knowledge of the ship and offshore welded structures subjected to ice-induced fatigue loading at seasonal sub-zero temperatures. The assessment of the fatigue loads produced by the interaction of the ice with ship and offshore structures is quite complex, and, if these structures are made of ferritic structural steels, they may undergo a ductile-to-brittle transition (DBT) at the low temperatures in Arctic waters. To this day, the current standards and guidelines do not address the effect of the low temperature on the fatigue strength of steel-welded structures. An interesting review regarding the fatigue assessment approaches at sub-zero temperature was recently proposed in [25].

Thus, clear recommendations are required to guarantee that fatigue failures are prevented in welded structures. The design of welded structures is commonly carried out by means of rules which impose conservative values of the allowable stress or consider partial corrective factors to take into account possible defects, residual stresses, corrosion and so on. The recommendations of the current codes, such as International Institute of Welding [26,27] and Eurocode [28,29] and recognized by some of the most important Classification Societies of ships and offshore structures, are conservative as was demonstrated by Crupi et al. [30] and Fricke et al. [31]. Experimental fatigue tests were carried out to assess the S–N curve of butt-welded joints, made of AH36 steel, which is used in shipbuilding [30]. Figure 12 shows the comparison between the design S–N curves (survival probability  $P_s = 97.7\%$ ), obtained by the traditional procedure [30] and reported in the IIW Code [26,27], demonstrating the conservativeness of the standard.

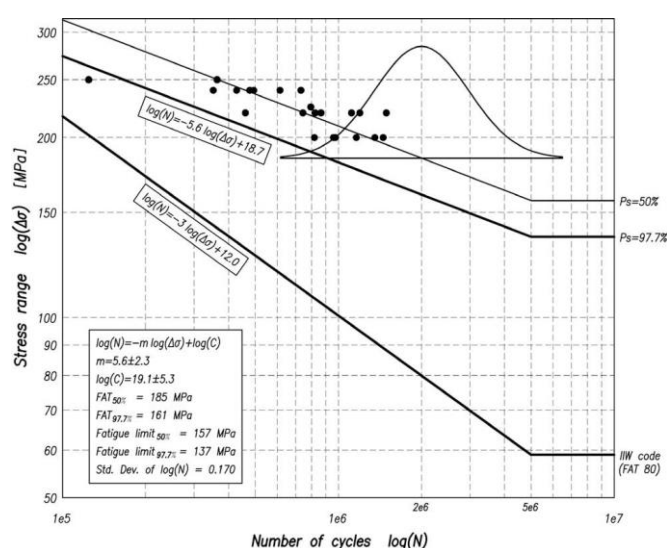


**Figure 12.** Experimental and design S–N curves [30]. Reprinted with permission from ref. [30]. Copyright 2021 Elsevier.

Fricke et al. [31] applied the fatigue assessment recommendations used by the Classification Societies for the fatigue assessment of a pad detail on the coaming of a Panamax containership, showing that numerous procedures, comprising the direct load design, produce very conservative results and the high scatter is due to different assumptions concerning load effects and local stress analyses and S–N curves.

The fatigue of welded joints is widely studied, and numerous approaches have been developed (Figure 13). An interesting review on fatigue of welded joints was given by Fricke [32].

The most common approaches include the following:

- The nominal stress approach [26,27];
- The structural approaches (structural stress approach [33], and the structural strain approach [34–36]);
- The local approaches (the notch stress intensity factor (N-SIF) approach [37,38], the notch strain approach [39,40], and the peak stress methods [41,42]);
- The fracture mechanics approaches (the crack propagation approach [43,44]);
- The energy approaches (the equivalent strain energy density (ESED) approach, and the averaged strain energy density (SED) approach [45,46];
- The critical distance methods (CDMs) [47–50];
- The thermal methods [50–55].

Some of them were improved when the evaluation becomes more complex and a multiaxial stress state occurs [43,56–61].

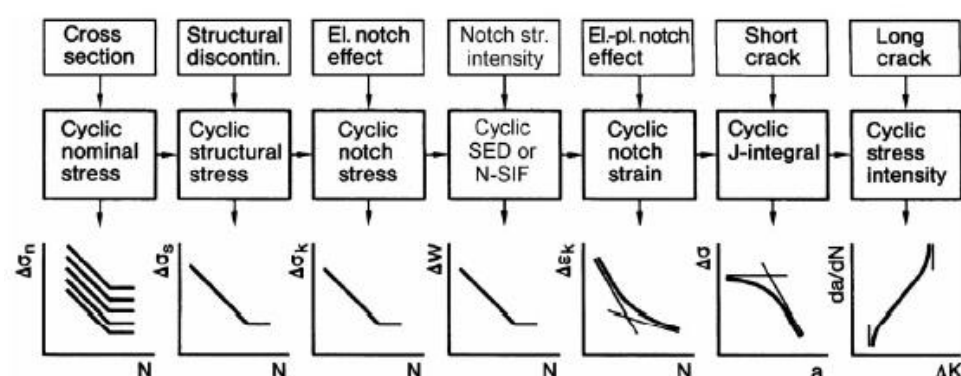


Figure 13. Global and local approaches for fatigue assessment of welded joints [26].

Recently, the abovementioned approaches were further assessed with several contributions, i.e., the cyclic structural stress was further developed by Dong [62,63] and extended in terms of structural strain of the LCF assessment [64,65], the elastic notch effect was reviewed in [66], the notch stress intensity approaches were deeply discussed in [66–68] and the peak-stress method was validated for many kinds of joints and was related to the SED and NSIF approaches [67,69]. In addition, Garbatov proposed a modified method [70] of the notch-strain approach.

However, there are not many other dedicated review studies to marine applications.

The present paper has the aim of giving a summary of the recent advances of the most used fatigue life prediction approaches and their applications in offshore and ship structures. The approaches were compared, considering that each approach has advantages and disadvantages. The comparison was based on a criterion which takes into account the applications. New insights, obtained by this comparison, were proposed, aiming to extend the service life of ship and offshore welded structures subjected to fatigue loadings. As reported above, the fatigue analysis of ship and offshore welded structures is a complex task, so the choice of the fatigue assessment approach depends on the specific application.



In addition, the future research direction regarding welding of dissimilar metals and autonomous welding methods are presented.

## 2. Approaches for Fatigue Assessment of Marine Welded Joints

### 2.1. Nominal Stress Approach

The nominal stress approach [26,27] assumes a total elastic behavior and that the S–N curves of welded joints with distinct geometries have the same slope for a specific material. In this case, a matching FAT (fatigue class), intended as the fatigue strength at  $2 \times 10^6$  cycles, is assigned. This kind of approach, which involves evaluating the fatigue strength by means of traditional fatigue tests, is considered in the current standards and recognized by the main ship classification societies. It ignores the effect of local stress increases due to structural discontinuities and local weld profile but includes the effects of the macrogeometric shape of the component in the vicinity of the joint, such as large cut-outs.

The nominal stress approach was applied in [71], where a considerable series of specimens made of DH36 steel and welded by means of the friction stir process was analyzed. The obtained S–N curve was compared to those recommended by the International Institute of Welding for fusion butt welds. In this case, a higher fatigue strength, corresponding to a higher FAT class, was found for the investigated marine grade steel.

The nominal stress method is particularly applied to simplify more complex problems, i.e., in the case of multiaxiality, as was done in [72]. In this case, a selection of codes and multiaxial fatigue methods for the marine industry were investigated, considering (non-proportional) constant amplitude loading, using nominal stresses. The authors concluded in [72] that there are large discrepancies between the applied codes (Eurocode, IIW and DNV-GL) and that the use of more local stress information could improve the results.

The nominal stress approach, even if it can provide significant dispersion and sometimes not very accurate results, is principally employed when the problems dealt with are particularly complex and other approaches are hard to be applied. Moreover, the nominal stresses are not always easy to be evaluated in the real welded structures with complex geometries, such as in the laboratory specimens.

### 2.2. Structural Approaches

The structural stress (alternatively ‘hot spot’ structural stress approach) has been defined in various ways: the mean stress value evaluated at certain distance away from the weld toe [32,73] or multiplying the nominal stress range by an appropriate stress concentration factor.

Generally, the structural hot spot stress, which does not take into account the effect of a notch radius, is determined through FE analyses and the procedures employed to assess the hot spot stresses, for the various types of hot spots, by means of finite element models, were firstly created for strain gauge use.

The structural stress approach usually uses idealized, perfectly aligned welded joints. This means that any potential misalignment has to be taken into account by the FEA model or by a proper stress magnification factor. Different variants of the approach exist which consider, for example, the effect of the stress gradient in the plate thickness direction and the plate thickness effect [33].

A method centered on the computed stress value 1 mm below the surface in the direction relating to the expected crack path was developed by Xiao–Yamada [74]. The total stress distribution along the crack path is the sum of the geometric stress produced by the structural geometry change and the non-linear local stress generated by the weld itself. The authors stated that, if compared to the surface extrapolation technique for structural hot spot stress evaluation, their proposed method [74] has the additional advantage of being able to consider the size and thickness effect observed in welded joints. Figure 14

shows the structural stress–life curve of the cruciform welded joint with various geometries [63].

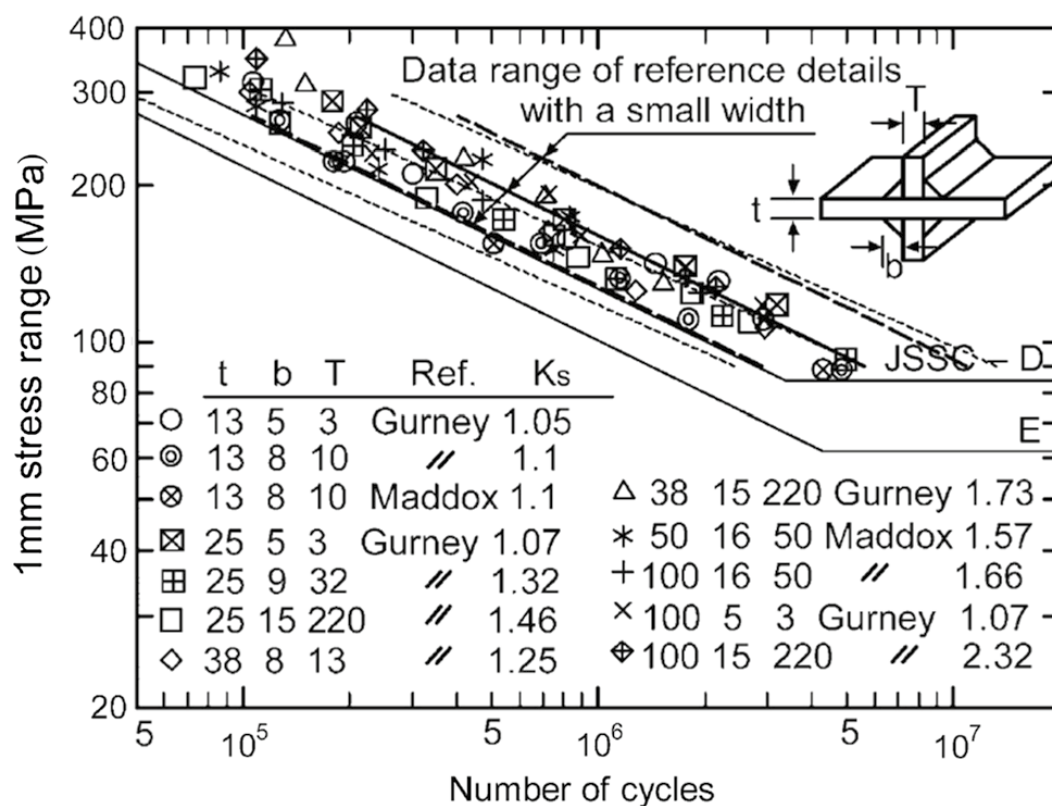


**Figure 14.** Structural stress–life curve of cruciform welded joint with various geometries [74]. Reprinted with permission from ref. [74]. Copyright 2004 Elsevier.

A different hot-spot stress method was applied in [75], using five typical welded joints widely used in ships, and offshore structures were analyzed employing five different solid element types and four different mesh sizes. The procedure was applied also to the more complicated pontoon–column connection part of a semi-submersible RIG under a representative wave load. The traction stress was defined at 0.5 t and 1.5 t away from the weld toe and was calculated using either a force equivalent or work equivalent approach, both of which are based on the internal nodal forces on the imaginary cut planes.

An interesting study comparing the fatigue strength assessment procedures used by the classification societies was performed by Committee III.2, ‘Fatigue and Fracture’, of the International Ship and Offshore Structures Congress (ISSC’2000) in Fricke et al. [31]. A pad detail on the longitudinal coaming of a Panamax container, shown in Figure 15, was chosen because of the well-defined loading due to hull girder bending. The authors concluded that the hot-spot that SCF derived varies considerably, and there are large discrepancies in the fatigue life predictions, ranging from 1.8 to 20.7 years. The spreading of results is attributable to assumptions regarding loads, local stress determination and the S–N curve. The hot-spot SCF derived varies considerably.

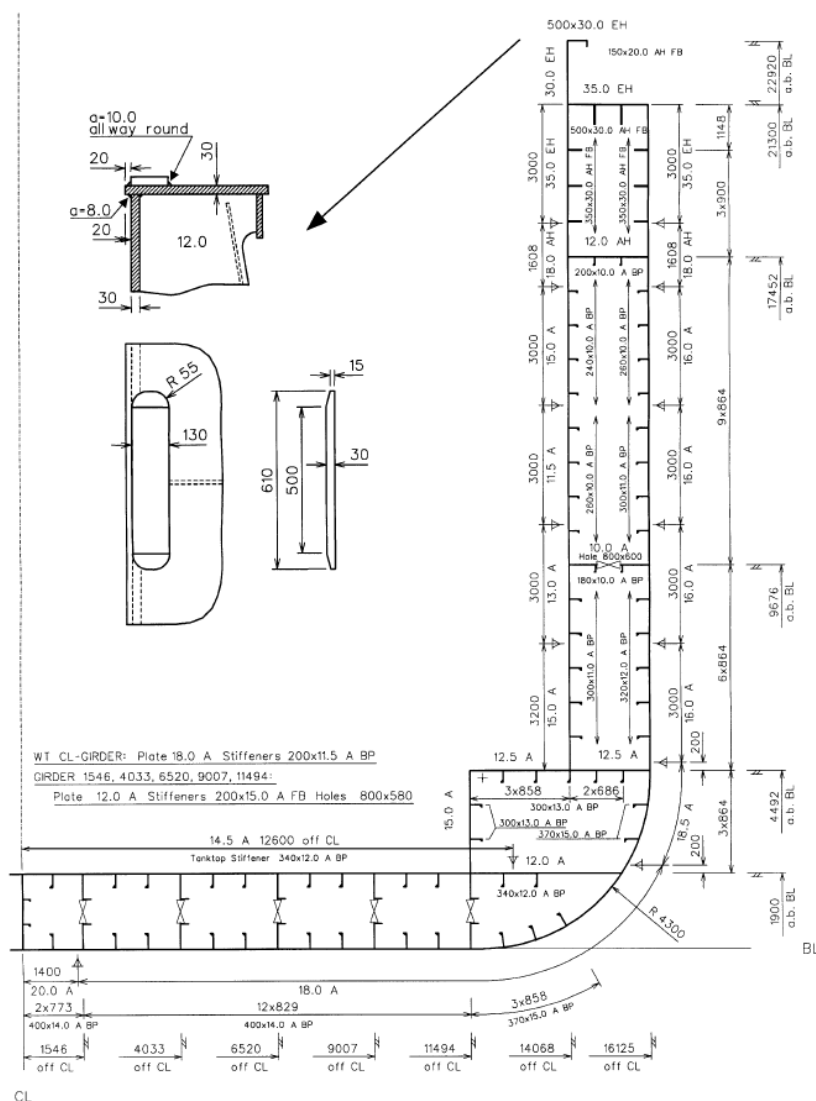


**Figure 15.** Detail of the longitudinal coaming of a Panamax container analyzed by Fricke et al. [31]. Reprinted with permission from ref. [31]. Copyright 2002 Elsevier.

The hot-spot stress was applied by Maddox in [76], who analyzed the structural details for floating production, storage and offloading (FPSO) units, where a high risk of weld toe fatigue failure occurs. Three different ways of determining the hot-spot stress, for different types of hot-spots, were assessed: by extrapolation from stresses 0.4 t and 1.0 t (IIW) or 0.5 t and 1.5 t (Classification Societies) from the weld toe, and as the stress 0.5 t from the weld toe. The authors concluded that the FAT 90 design of the S-N curve is suitable in all three cases, but FAT 80 would be more proper for structural details that exhibit high stress gradients moving toward the weld toe, especially with hot-spot stresses calculated at 0.5 mm from the weld toe. However, the results were influenced by a high dispersion and the unavailability of all the three definitions of hot-spot stresses of the investigated weld details.

Structural details of FPSOs units, applying the hot-spot stress, were investigated also by Fricke et al. [77]. Five distinct details (some of them used also in shipbuilding) with different geometry and fatigue loading, were selected, for which stress measurements and fatigue tests are available. The authors used different FE programs, FE models and different mesh size and element types, applying three different stress extrapolation techniques depending on the plate thickness. The derived hot-spot stresses and the estimated fatigue lives were matched with the existing design of S-N curves of the International Institute of

Welding (IIW), concluding that the hot-spot stresses predicted using the three stress extrapolation techniques are suitable with the current design of S–N curves.

Nevertheless, as previously observed, the nominal stress and hot-spot stress approaches have some limitations regarding the thickness effect consideration and are sometimes conservative due to the high dispersion. Furthermore, the design of the S–N curve can be very subjective because the weld classification is based on the dominant loading mode and the mesh size and not only on the joint geometry. Within this context, Dong [63] proposed a new definition of structural stress which is not mesh sensitive, later applied on various ship welded joints, by considering the gradient stress distribution along the welded plate thickness and establishing equilibrium equations from the elemental node forces. This new structural stress definition, calculated on the potential crack path is based also on the division of the normal stress into the membrane stress and bending stress, resulting in the effect of the loading mode being able to be taken into account. Thus, the new structural stress approach can consider different geometries subjected to different loading modes, different thicknesses, and misalignment effects, and it is not mesh sensitive [33,63], being more advantageous with respect to the traditional hot-spot structural stress.

The S–N curve obtained by the equivalent structural stress proposed by Dong is compared to a master S–N curve, in a narrow scatter band, as shown in Figure 16 [78].

Dong's approach of the equivalent structural stress was successfully applied to the orthotropic steel deck (OSD) [63,79], widely applied in shipbuilding [80]. OSDs are exceptionally common in the ship building industry and for hydraulic purposes such as tanks, gates, and locks. In [62,79] it was concluded that the mesh insensitive traction-based structural stress definition is efficient for describing the relevant stress state responsible for each of the fatigue failure modes. The same approach was successfully extended through a formulation of an effective equivalent structural stress transfer function in order to incorporate multiaxial non-proportional loading conditions, for the assessment of marine structures exposed to time-varying loads, in [81].

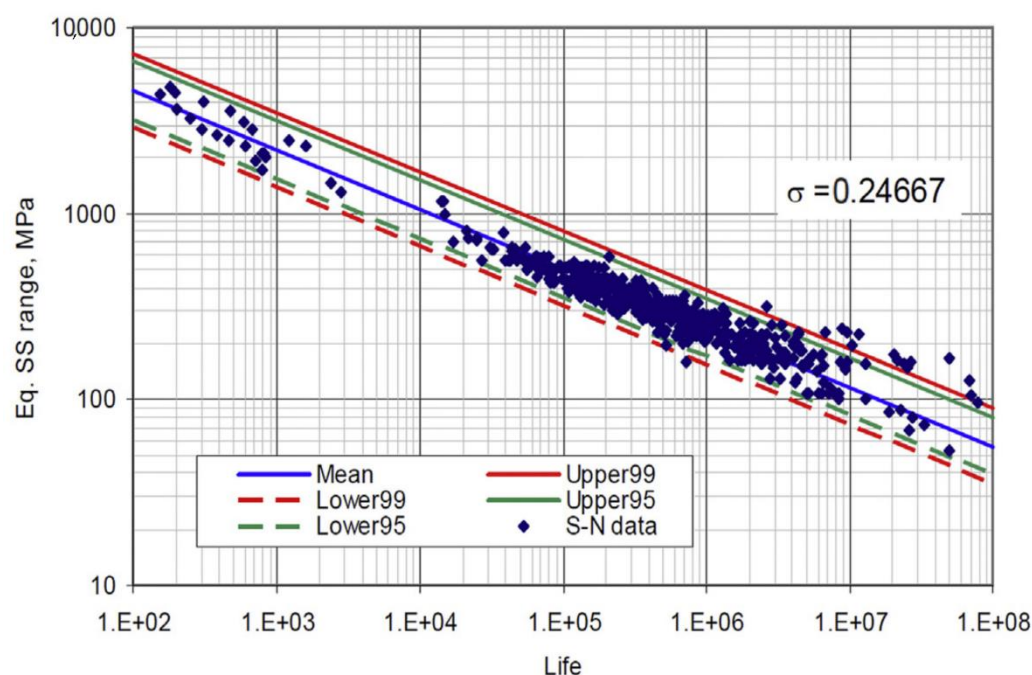


**Figure 16.** Master S–N curve obtained from Dong's structural stress [78].

Furthermore, for fillet-welded specimens, based on typical shipbuilding practices, the weld penetration effects on the fillet weld load carrying capacity were investigated in [82]. It was noticed in [82] that both an effective weld throat stress-based criterion by

combining normal and shear traction stresses and an equivalent effective stress-based criterion based on the master S–N curve formulation can be applied for the evaluation of the minimum fillet weld leg size beyond which weld toe fatigue failure dominates.

Recently, Dong and co-authors proposed an extension of the structural stress approach for the low-cycle fatigue life prediction, using a structural strain parameter capable of correlating both LCF and HCF fatigue data of welded structures [35,65].

The structural stress and structural strain methods were particularly used in an ill-defined weld toe [27,34,35,63,65,83]. The equivalent structural strain was applied by Dong and coauthors to girth-welded offshore pipes, considering the cyclic nonlinear behavior [78] which influenced the LCF behavior. However, it is worth noting that if the experiments are displacement controlled, the structural strain can be calculated through a linear elastic model [64,65]. Deeper analyses on the structural strain approach can be followed in [35,64]. The results of the equivalent structural strain approach can be compared with a master E–N curve representing over 1000 large scale fatigue tests [83], with the cycle to failure ranging from  $10^2$  to  $10^8$ . Actually, there are two Master S–N curves in the ASME code, with one for steel and one for aluminum. However, as shown in ref. [65], LCF fatigue data using the structural strain approach and fatigue data of different metals (data from cruciform fillet-welded specimens consisting of two types of aluminum alloys used in shipbuilding, two types of titanium alloys and ship hull steel) can be collapsed in a single master E–N curve. Furthermore, the validation on a ship structural detail and 63 ship hull steel specimens of the structural strain approach was reported in [65] and is shown in Figure 17.

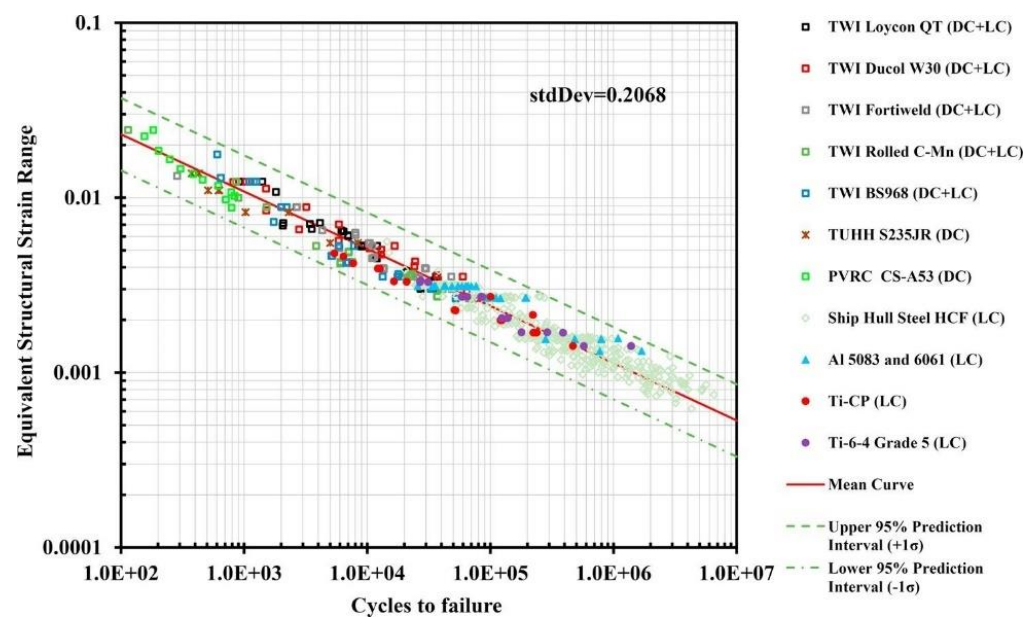


**Figure 17.** Equivalent structural strain range versus cycle to failure: fatigue test data analyzed in [65]. Reprinted with permission from ref. [65]. Copyright 2019 Elsevier.

A new experimental approach, based on the digital image correlation (DIC) technique, for the structural strain evaluation in LCF condition of welded joints was firstly proposed in [84]. The DIC is an experimental technique extremely useful for detecting very high local displacements and strains and permits a deep analysis of the mechanical behavior of welded joints, as shown in [85]. The new approach, namely “DIC-based equivalent structural strain approach”, is related to the definition given by [35,65], but it was evaluated on the specimen surface instead of thickness. The DIC-based structural strain approach was applied successfully for predicting the LCF life of AA 5083 welded joints, used for shipbuilding and marine structures [84]. The equivalent DIC structural strain

results were compared to the ASME mean curve [83], representing over 1000 experimental data, showing good agreement.

The structural stress approaches are generally more accurate than the nominal stress approach, thus are preferable. However, a distinction of the different kinds of structural approaches should be considered. The hot-spot method is often used and has some drawbacks as different FAT classes based on geometry and loads; furthermore, fine meshes are needed at weld toes. One of the most interesting stress approaches is the equivalent structural strain proposed by Dong, which overcomes the FAT classes selection and is mesh insensitive. In addition, it can be easily applied also for low-cycle fatigue life prediction, transforming the structural stresses into structural strains. This approach looks very useful, as it could be applied for a large-scale structure since the assessment of the entire structure and not only of the specimen will be more and more required in future ships and offshore structures design.

### 2.3. Local Approaches

The notch stress approach is a suitable approach for the fatigue assessment of welded ship structural details. Compared to the nominal and the structural hot-spot stress approaches, it offers the possibility to explicitly take into account the local weld geometry. Thus, it can take into account the stress concentrations caused by the geometry of the detail, as well as the thickness effect, and by the local weld toe or root radius. The notch stress method contemplates a perfect elastic behavior, and one of its main advantages is given by the possibility of representing a given type of material by means of a single S–N curve.

Relying on the quality, which is revealed by the cutting procedure and potential post treatment, such as grinding, FAT classes between FAT 100 and 160 are used for ship structural steel welded joints in [27,86].

A so-called effective notch stress approach (ENSN) was proposed [87] for the fatigue assessment of the welded joints. The concept of the effective notch radius implies that the profile of the weld toe is replaced by a rounded notch with a specific radius, then the stress concentration factor  $K_t$  around the notch can be calculated by FE analysis.

In order to consider the microstructural support effects of the material in the relatively sharp notches of the weld toe or root, Radaj's approach [87] assumes a fictitious radius (reference radius) of  $r_{ref} = 1$  mm and an actual radius of zero in order to be conservative. Detailed discussions can be found in [88].

The size of the effective notch radius depends on the thickness of the welded plates, so it was proposed in [89] to adopt a specific ratio of two dimensions: the radius and a dimension of the weld.

A coarse mesh is usually applied far from the singularity zone, while a finer mesh is used in proximity of the local weld radii as acknowledged in the IWW documents [88]. Exhaustive features of finite element modeling were analyzed by Fricke [88]. FAT 225 has been recommended for the S–N curve design of steel structures, using the effective notch-stress approach, analyzing ship welded joints [27,73,86].

Fricke and Kahl [90] examined four large-scale test models, in HCF conditions, which had two bracket connections and bulb plate stiffeners. The notch stress approach results were determined considering an enlarged toe radius, a nominal and the fictitious radius of 1 mm (worst case approach). Furthermore, the structural hot-spot stress was estimated according to the IWW fatigue design recommendations. The authors [90] concluded that considering the worst case (1 mm fictitious radius) resulted in conservative calculations in relation to the recommended IWW design S–N curve (FAT 225). The realistic weld profile with an enlarged weld toe radius resulted in smaller notch stresses, and lower S–N curves should be used. In addition, the notch stress approach gives better fatigue predictions compared to the hot-spot stress approach.

The effective notch stress approach was applied for analyzing the stress distributions and the fatigue damage of the welded joint at two hot spots of the double hull oil tanker



structural detail, and the fatigue damage assessment, accounting for corrosion deterioration of the considered hot spots, was considered [91].

In the case of large deformations, the notch stresses could be converted in terms of notch strain values. Thus, the notch strain approach is certainly suitable for low-cycle analysis. Generally, the cyclic elastic–plastic material properties have to be priorly known, and they refer to the crack initiation life obtained from experimental tests. Detailed discussion can be found in [87]. The notch strain approach was further improved by Sonsino [33,92] with regard to the multiaxial fatigue of welded joints.

The effective notch strain (ENSN) approaches were applied for the detection of the crack initiation by Saiprasertkit et al. [39,40] to cruciform welded joints used in steel bridges and offshore platforms [93], who described the fatigue life as the number of cycles when the maximum load dropped by 20% due to crack propagation.

The effective notch strain ENSN method was positively used to detect the fatigue crack initiation of load-carrying cruciform joints [94]. Fricke et al. [95] analyzed the LCF strength of welded joints in ship structures, proving the effectiveness of the ENSN approach.

The notch strain approach was applied on typical butt-welded joints used in ships in [96], incorporating the effect of misalignment, secondary notch, residual stress and fatigue limit. The authors also developed a strain-based fatigue reliability assessment using a probabilistic distribution for the low-cycle fatigue stress range.

The limits of the ENSN are due to the difficulty of using elastic–plastic material properties that are not always priorly known, and relative fine meshes are required, which makes this method not very suitable for large-scale structures, unless the submodeling technique is adopted.

The notch stress intensity approach (N-SIF) defines the stress intensification at a notch tip and can be employed to evaluate the fatigue crack initiation life of notched elements. Lazzarin and Tovo [37] developed a notch stress intensity factor (N-SIF) approach for welded joints achieving good quality results on various welded joints, in terms of S–N curves. The region surrounding the weld toe is modeled as a sharp V-notch, and the results are generally correlated to mode I N-SIF. However, considering a zero radius at the weld toe can lead to an underestimation of the fatigue life [97]. The initiation phase is hardly separable with respect to the initiation phase; detailed discussion on the propagation approaches can be found in [98].

Some SIF formulas for welded joints are available, and they are generally restricted to simple basic weld joint shapes (e.g., butt joint, T-joint, and cruciform joint). Although ship components could be considered to be made of several simple joints, still the stress distributions in real ship details are more complex than those of simple joints because of the load flow in the structure near the detail as well as the local stress concentration influence. As reported in [99], when complex ship components are assessed using stress intensity factor formulations for simple welded joints, the global nominal membrane stresses and global nominal bending stresses must be revised with a stress concentration factor that considers the gross structural configuration surrounding the detail, and a stress concentration factor that considers the difference between the stress concentration of the detail's configuration.

In addition, when dealing with marine structures, often, NSIF calculation methods are complemented by the influence of wave loads. The prediction of fatigue crack growth in a ship detail under wave-induced loading was discussed in [20]. The authors applied a FE model procedure to assess the SIF in complex ship structures by using a coarse mesh in the FE model of the whole ship and refining the mesh within a sub-model of the most stressed welded joint. Furthermore, a procedure of generating the fatigue loading spectrum based on a design wave approach was presented to face the challenge of the definition of nominal stresses [20], and the Paris law was determined.

A similar procedure was used in [100], where authors presented a complete work from hydrodynamic analysis to fatigue life prediction of a critical joint connecting cross

braces and pontoons of a very large floating structure (VLFS), concentrating on the SIF calculation. The spectral method was used for the creation of a loading spectrum and was employed for SIF calculation. The authors introduced also a fatigue crack propagation model and concluded that this approach is more consistent than the design wave approach, and the use of sub-model techniques significantly reduced the calculation burden.

The load spectrum obtained in [86] was used for SIF calculation and crack propagation evaluations, using submodeling techniques with refined meshes. The authors compared the results with some empirical formulas. In a similar way, a procedure for fatigue life prediction based on fracture mechanics and spectral analysis was applied to predict the crack growth of a very large floating structure in [100], where the SIF was calculated by means of the submodeling technique by FEA and through some existing empirical formulas in stochastic sea conditions.

The authors of [101] combined measured strain achieved at a monopile support structure of a 3 MW to calculate bending moments together with oceanographic data to predict the remaining fatigue life of offshore wind turbine support structures. The SIF range was evaluated, and the remaining fatigue life was calculated according to Miner's rule. Since the oceanographic data change from year to year, the authors concluded that the proposed methodology can be applied, and the remaining life of monopile support structure of offshore wind turbines can be updated each year. However, as mentioned, the main limitations of the SIF approach are that 1) considering a zero radius at the weld toe can lead to an underestimation of the fatigue life [97]; 2) the initiation phase is hardly separable with respect to the initiation phase, and detailed discussion on the propagation approaches can be found in [98]; 3) some SIF formulas for welded joints are available, and they are generally restricted to simple basic weld joint shapes. Although ship components could be considered to be made of several simple joints, still the stress distributions in real ship details are more complex than those of simple joints because of the load flow in the structure near the detail as well as the local stress concentration influence.

Another approach, which is the peak stress method (PSM), that permits to use coarser meshes for the estimation of the NSIF was proposed by Meneghetti et al. [41,42]. The authors found that the correlation between the NSIF and peak stress was constant if the realized finite element model had a specific mesh pattern and fixed element size. Meanwhile, such a relationship should be calibrated before the assessment [41]. The calibration of the parameters used for the NSIF evaluation was performed with several 2D and 3D FEs and commercial FE codes [41,69,102]. Although the PSM has never been applied to welded joints for shipbuilding and offshore structure, to the authors' knowledge, the 3D modeling of large-scale structures, such as ships and offshore structures is increasing rapidly, pushing the need for more efficient and time-saving fatigue assessment approaches, and thus the 3D PSM could be applied in shipbuilding and offshore structures, as it requires relative coarse meshes.

#### *2.4. Fracture Mechanics Approaches*

Fracture mechanics approaches can be used for predicting the fatigue life of welded joints used for marine structures.

The fracture mechanics approaches are based on the prediction of the crack propagation using the Paris law, which correlates the crack growth rate as a function of the stress intensity range  $\Delta K$  and permits the assessment of the fatigue crack growth resistance of a material. The crack growth depends on several parameters: stress ratio, thickness, weld defects, and the environment conditions. Crack growth in salt water is significantly faster.

A new model for predicting the crack initiation and crack growth lives was developed in [103] by conducting corrosion fatigue tests on steel tubular T and Y joints used for offshore structures.

Sonsino [104] applied the crack propagation approach and other methods (structural stress, notch stress and notch strain approaches) for predicting the fatigue life of welded

offshore K-nodes and it resulted that all the approaches, except the notch strain approach, showed similar predictions, achieving good agreement with the experimental results.

The welded steel structures in marine and offshore constructions are generally subjected to variable amplitude (VA) fatigue loads. Their fatigue life depends on the level and sequence of the service load cycles, which can produce crack growth retardation or acceleration. Some fatigue tests were carried out on welded, thick-walled specimens, made of C Mn steel, which is used for offshore structures, and two fracture mechanics models (the Space-state model and the generalized Willenborg model) were applied in [105].

VA fatigue tests and fracture mechanics analysis, used for the assessment of the fatigue lives, were performed on full-scale offshore tubular joints in [106], demonstrating that Miner's rule, which is normally used in the design of steel structures under VA fatigue loads, is unconservative.

The fracture mechanics approaches have advantages and drawbacks. The main advantage is that the crack propagation life may be directly evaluated. A drawback is that the crack initiation life is ignored. Thus, fracture mechanics approaches should be used to complement other approaches. In addition, the accuracy is deeply affected by the mesh refinement; indeed, the mesh refinement changes the elements' capability to describe the singularity at the crack tip, and it needs an adjustment of the mesh at every crack growth increase.

## 2.5. Energy Approach

One of the limits of the ENSN is due to the difficulty of using elastic–plastic material properties that are not always priorly known. In this case, methods relying on elastic stress–strain behavior at notches, such as Neuber's rule [107] and the equivalent strain energy density (ESED) approach [107], could be used.

Dong and Soares [108] compared various analytical approaches with elastic–plastic FE analysis and concluded that the plane strain ESED approach works well. As reported in [70], the ENSN range can be determined making use of the plane strain ESED approach, which involves as inputs the nominal stress range, the material cyclic strength coefficient and the cyclic strain hardening exponent. The cyclic strain hardening exponent are employed to describe the cyclic stress–strain curve. The procedures of estimating the ENSN range, proposed in [108], were validated, reanalyzing some published experiments performed in the LCF regime [13,70,109]. These experiments were chosen because the material properties, such as  $K'$  and  $n'$ , are available.

The comparisons gave reasonable results, and two different curves for LCF and HCF were given, as reported in Figure 18.

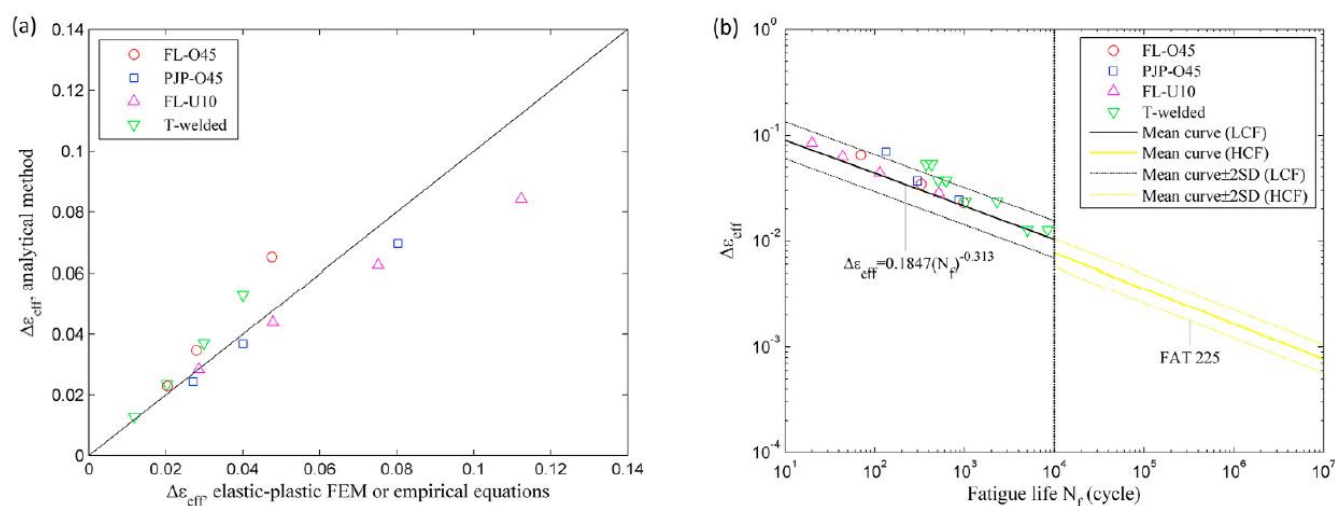


**Figure 18.** Results of procedures of estimating the ENSN range, proposed in [70]. (a) ESED approach vs elastic-plastic FEM or empirical equations; (b) ENSN ranges estimated by ESED approach plotted against fatigue test results. Reprinted with permission from ref. [70]. Copyright 2021 Elsevier.

To overcome the shortcomings of NSIF-based approaches, such as the need for FE models with extremely sophisticated meshes [110], the dependence on the notch opening angle [111], and the underestimation of the fatigue life by considering a zero radius at the weld toe [97], averaged strain energy density (SED) based models were developed. Lazzarin and co-authors [45,46] proposed a new approach, centered on the mean value of the strain energy density (SED) in a control volume of radius  $R_c$ , which is reliant on welded material properties, near the weld toe or the weld root. Fischer et al. [66] reviewed the design of the S–N curves of the N-SIF and SED approaches considering the misalignment effects in welded joints used in marine structures, which should be integrated on the load side of local approaches in order to consider them independently in different types of welded joints used in ships. More features about the averaged strain energy density approach can be found in the works by Berto and Lazzarin [112,113].

The SED approach was applied in [114] for welded joints used in ships and offshore structures subjected to Arctic environments. In particular, the SED method was extended for the fatigue assessment of welded joints at sub-zero temperatures in [114], performing also fatigue tests of welded joints, made from normal and high-strength structural steel in the span of 20 °C to −50 °C. The obtained results were compared with results of studies on the SED-based assessment of notched components at high temperatures. Within this context a temperature modification function for SED was proposed by the authors for design purposes.

## 2.6. Critical Distance Methods

The critical distance approaches describe failure conditions based on the hypothesis that the failure of a structure occurs when the fatigue limit is surpassed within a region bordering the notch (critical volume) and not in a local single point. The critical distance, according to Taylor [48], can be expressed in terms of a material length parameter,  $L$ , that is defined in terms of the plain specimen endurance limit  $\sigma_{th}$  and the fatigue crack propagation threshold  $K_{th}$ . More details about the theory of critical distance, TCD, can be found in [115].

The critical distance method CDM was successfully applied in [49,50] for T weld joints made of AA5083 aluminum alloy, extensively used in ship structures. The endurance limit was evaluated by means of the TCD, from finite element analyses (FEA), obtaining good estimates of the fatigue strength validated by experimental data. TCD is a relatively simple approach since it implies a perfectly elastic approach. However, like elastic fracture mechanics, it is not likely to work under general plasticity conditions, or any conditions which require a relatively small plastic zone compared to the nearby elastic region. The brittle-to-ductile transition is generally linked with a loss of constraint (plane strain to plane stress transition). Sometimes a loss of constraint can take place as the notch radius increases, due to the higher applied stress before fracture. In this case, the failure occurs after widespread yield and no longer matches the TCD predictions obtained for the plane strain. However, the TCD prediction can also be performed for plane stress conditions, thus the result of constraint loss should be integrated into the TCD.

Susmel [116] applied TCD along with the modified Wöhler curve method (MWCM), a critical plane approach, to estimate the fatigue life of steel and aluminum welded joints subjected to multiaxial fatigue loading.

## 2.7. Thermal Methods

As reported in [117], the thermal methods [118–127], which are based on the detection of the self-heating effect of the metallic materials subjected to fatigue loading using the thermographic technique, can be classified into several categories.

The thermographic method (TM) [118] is based on the assumption that the fatigue strength can be evaluated as the highest stress level that produces no temperature increment on the surface of a specimen subjected to fatigue loading. The TM and the energy approach [119] permit a faster determination of the fatigue strength and the S–N curve of materials and welded joints compared to traditional fatigue tests.

As reported above, the real structures are subjected to VA fatigue loads, so the quantitative thermographic method (QTM) [53] was developed in [117]. Then it can be applied to marine and offshore structures, which are subjected to VA fatigue loads during their service lives.

The thermographic methods were applied by the authors for the fatigue assessment of the following welded joints used in ship and offshore structures: AA5083 T-welded joints [50], butt-welded AH36 steel joints [30], butt-welded AH36 steel joints with different thicknesses (from 5 to 20 mm) [15], butt-welded AH36 steel joints with defects [128], butt-welded S355 steel joints [129], AL/FE explosive welded joints [130], and Ti6Al4V/Inconel 625 laser welded joints [131].

As already mentioned, the energy approach [119] allows the assessment of the S–N curve, and it was applied to three butt-welded AH36 steel specimens in [30]. Figure 19 shows the S–N curves (survival probability  $P_s = 50\%$ ) predicted by the energy approach and obtained in accordance with the traditional procedure for a comparison. It results that a good agreement is achieved, and the scattering of the S–N curve parameters ( $m$ ,  $\log C$ ) predicted by the energy approach is lower than that of the traditional S–N curves [30].

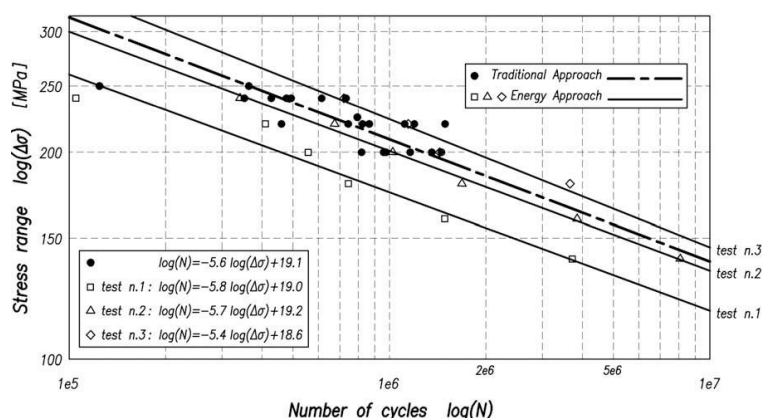


**Figure 19.** S–N curves obtained by traditional and energy approaches [30]. Reprinted with permission from ref. [30]. Copyright 2021 Elsevier.

The four types of butt-welded AH36 steel joints, investigated in [128], differed for the presence of weld defects and for thickness values. The evaluation of the defects inside the investigated butt-welded joints was performed using 3D computed tomography (CT), which allowed the measurements of cumulative defects volume ( $V$ ) and maximum defect size ( $D_{MAX}$ ). Figure 20 shows the CT analyses of a welded specimen.

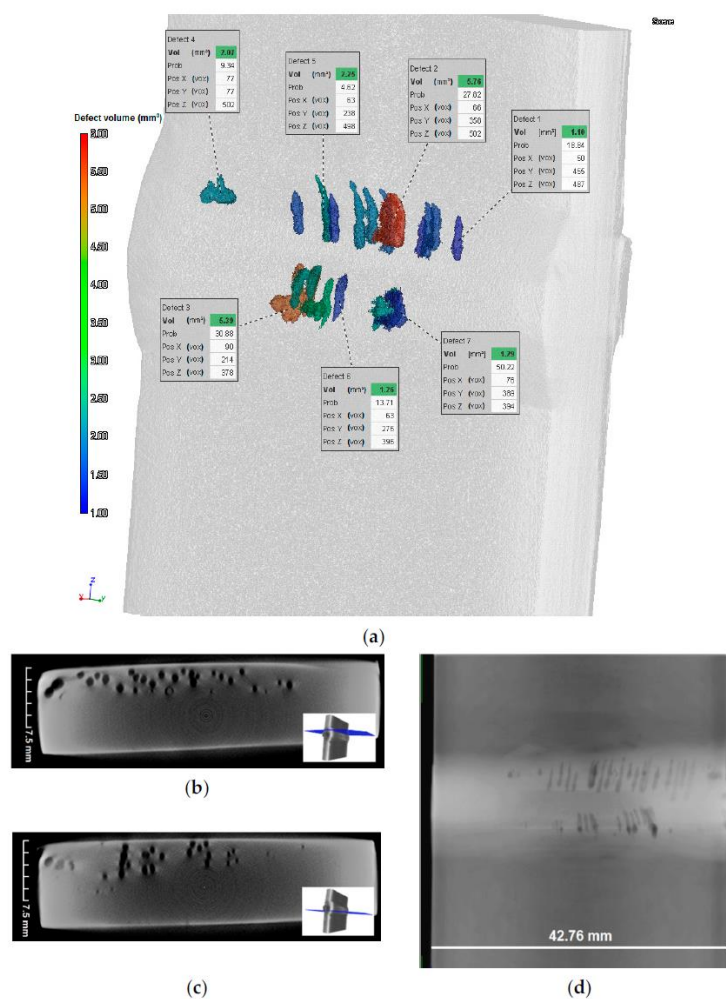


**Figure 20.** CT results for a specimen: (a) defect evaluation; (b,c) tomograms of the cross section of the weld bead and (d) some along X-rays of the joint. [128].

The analysis of the thermographic images allowed the assessment of both the fatigue strength of the welded joints, applying the rapid thermographic method, and the S–N curve by the energy approach [128].

Figures 21 and 22 show the values of the fatigue limits predicted using the energy approach ( $\Delta\sigma_{e\Phi TM}$ ) versus the cumulative defects volume ( $V_N$ ) and the maximum defect size ( $D_{MAX,N}$ ), normalized with respect to the thickness of the welded joints.



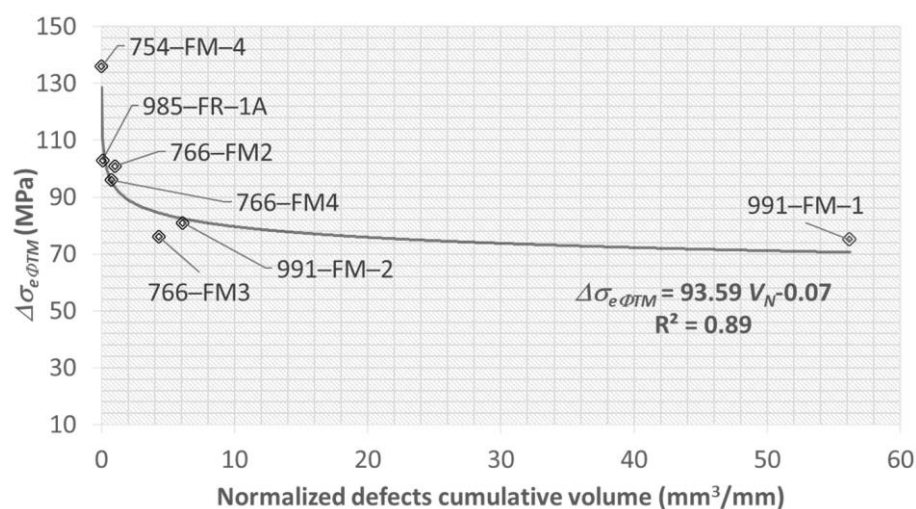


Figure 21. Fatigue strength ( $\Delta\sigma_{e\Phi TM}$ ) vs. normalized defects cumulative volume ( $V_N$ ) [128].

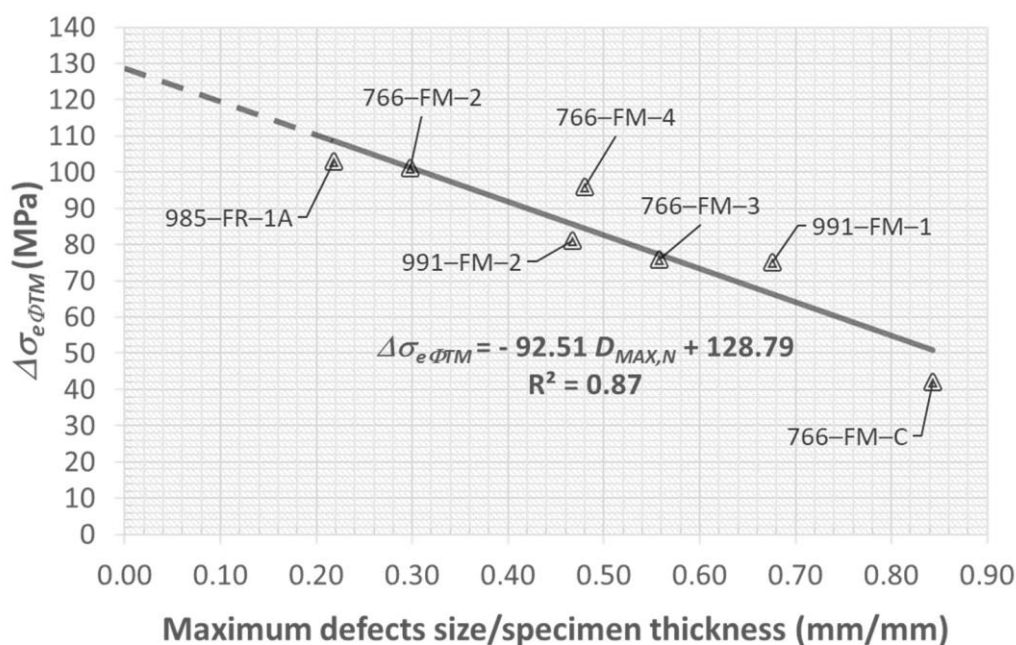


Figure 22. Fatigue strength ( $\Delta\sigma_{e\Phi TM}$ ) vs. normalized maximum defect size ( $D_{MAX,N}$ ) [128].

Micone and De Waele [132] developed a methodology, based on the direct current potential drop (DCPD) technique, for a rapid assessment of the S–N curves of two high strength offshore steels and compared the so-obtained S–N curves with the ones obtained by the application of the thermographic technique, achieving a good correlation.

The thermal approaches are particularly suitable and give fast prediction for the fatigue life of welded structures, especially the rapid thermographic method that theoretically predicts the entire S–N curve with only one specimen. However, at least three specimens should be investigated to consider dispersion and to avoid that the prediction is made totally considering one specimen that could include defects due to the welding process. The disadvantage is that these approaches are rather experimental than numerical.

### 3. Future Developments of Welded Joints in Marine Structures

Nowadays, the need for using different materials to optimize the weight and structural performance of ships and marine structures is rapidly increasing. Within this

context, the challenge of joining different materials denotes an essential task. The prevalent type of dissimilar welded joints employed for shipbuilding and offshore applications is represented by the Al/Steel type joint (Figure 23).

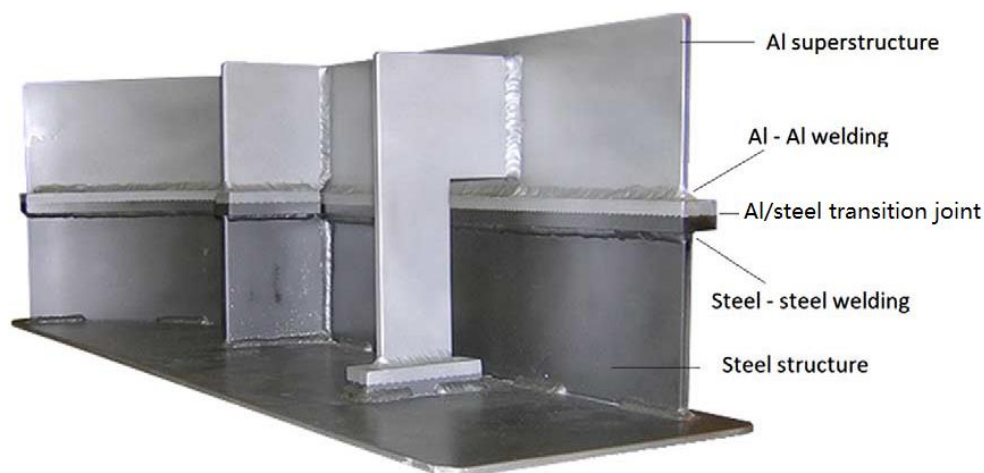


**Figure 23.** Example of an Al/Steel EW joint in shipbuilding.

An example of steel hull to Al superstructure connection is shown in Figure 24, where bimetallic strips were used between the boat's hull and upper section [133] in order to weld the steel hull side on the to the steel side and the aluminum upper section to the al side of the bimetallic joint.

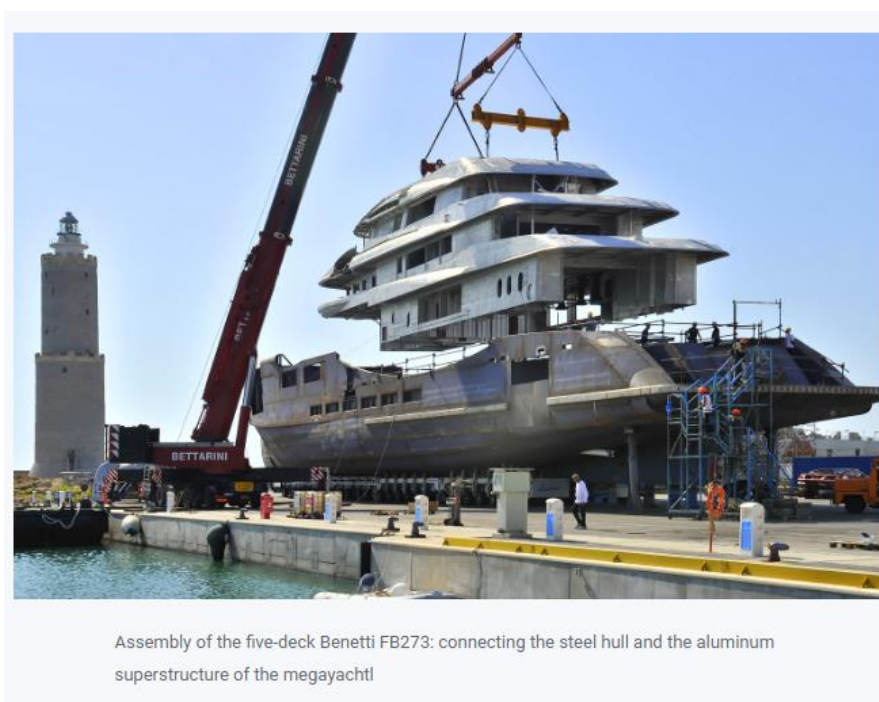


**Figure 24.** Welding steel hull to Al superstructure [134]. Accessed date 26 February 2022.

Iron has low solubility in solid aluminum and forms a eutectic with aluminum. Moreover, aluminum is a decent deoxidizer and is employed in reduced amounts in iron-based alloys. Thus, the traditional fusion welding of aluminum and iron-based alloys represents a technologically and science-intensive task. Still, using laser welding or welding–brazing, proper joints that meet the requests can be obtained. The mechanical properties of this kind of joints can reach a level of 70% of the utilized aluminum alloy [135]. Some studies

about the implementation of friction stir welding [136] and laser welding [137] exist. However, the joints produced by FSW [136] seem to give a nonuniform distribution of the mechanical properties, and the fatigue life of laser-welded joints still needs to be fully evaluated [137]. The evaluation of the current literature informs that the main four tasks to be handled in aluminum/steel welded joints are [57] reducing intermetallic compounds (IMC) at the interface, monitoring the thickness of IMC layers to avoid the advance of brittle phases, avoiding the formation of pores and cracks which lessen the global strength of aluminum/steel welded joints, and the employment of advanced mechanical characterization methods to assess and consider the non-uniformity of mechanical properties in the joint.

Due to the difficulty of connecting aluminum to steel by means of the traditional welding technique, the most reliable welding technique appears to be explosion welding (EXW), which provides a solution for the shipyard fabrication of reliable aluminum–steel structures. The explosion welding (EXW) method is a solid-state welding technique that employs the high energy of explosives to cold weld two dissimilar metal parts. The metals are bonded due to plastic deformations that take place at the collision front of the metals faces by means of a chemical explosive charge. Various experimental studies are described in the literature [130,138–140]. The interface morphology and weld strength deeply depend on impact velocity and impact angle [130], and it is very common to use an intermediate plate due to the difficulty of directly welding aluminum alloy and steel. Corigliano and co-authors investigated Al/Steel explosion welded joints for shipbuilding and offshore structures, made of three layers [130]. The work reported experimental three-point bending fatigue tests, confirming the good quality of the investigated joints.

Experimental analyses of S355J2+N steel and AA5083 aluminum alloy welded structural joints employing explosion welded transition joints were performed in [138], showing that the strength of the welded joint resulted in being equal to 87–95% of the base material (AA5083) strength; furthermore, rupture never occurred in the explosion welded joint but only in correspondence of the Al/Al welded zone, confirming once again the reliability of the EXW transition joints. However, it should be highlighted that a higher thickness of the EXW transition joints was used for the experiments, according to the recommendations of the major classification societies and clad producers.

When other properties, such as higher fatigue and static strength [141], enhanced corrosion resistance [142,143] and weight reduction, are needed for offshore and oil and gas structures [141], further materials are used in marine environments [144,145]. For instance, titanium alloys, stainless steel alloys and Inconel alloys might be used in the same circumstance to minimize the weight and improve the tensile and corrosion resistant properties [146,147].

The direct welding of Ti and Ni alloys produces various problems: the development of fragile compounds, high residual stresses, and segregation. The characteristic of the welded joints is greatly influenced by the development of brittle intermetallic phases, cracks and porosities. Furthermore, due to the variation in terms of thermal expansion coefficient between the two alloys, high residual stresses are produced during the welding process, which can decrease the fatigue performance of the joint. Further problems arise because of the different density and diffusivity, which imply a strong inhomogeneity of the joint.

Due to the above-mentioned difficulties to weld these kinds of dissimilar materials, only a few studies exist, to the authors' knowledge [131,148]; principally, Stainless steel-Inconel 625 joints [149] and Superduplex Stainless Steel/HSLA Steel [150,151] joints are currently applied for the offshore and oil and gas industries. A new Inconel 625/Ti6Al4V laser welded joint was investigated by Corigliano and Crupi in [131] who evaluated the fatigue strength and applied the TM. A new solution was proposed in order to avoid the problem of joining these two alloys and to achieve better weld quality: intermediate layers of vanadium and stainless steel were used. The fatigue strength assessed experimentally proved the good quality of the investigated joints and was in good

agreement with the value predicted by the TM. The value of the fatigue strength obtained is particularly promising, considering that it is even higher than the tensile strength achieved during static tests in [148].

New oil and gas exploration areas have pushed to further hostile environments, i.e., very deep-water offshore reservoirs, which require the growth of new technologies to guarantee safe and reliable operations. Within this context, the reel-lay method looks like an efficient technique employed for the installation of subsea pipelines and risers. The main advantage is given by the possibility of onshore welding and inspection of the pipeline, which permit high quality welded joints compared to traditional laying techniques. In addition, a better solution toward the corrosion resistant behavior can be taken. In particular, the use of clad and lined C-Mn steel pipelines, including X65 and X70 grade steels, with a thin interlayer of corrosion resistant alloy (CRA), is becoming frequently adopted to assure the essential resistance against corrosion [152].

Dissimilar welded joints are often employed in offshore nuclear power plants, with one or more nuclear reactors that can be positioned on a platform at sea [153]. The world's first floating nuclear power plant was built at the Baltiysky Zavod shipyard in Saint Petersburg. It is an independent site that can supply electricity and heat to zones with difficult access and, thanks to sea water that absorbs the movements of the sea floor, safeguards the plant from earthquakes and tsunamis [154]. As reported in [155], the main building materials of light water reactors (LWR) are low alloy steels, stainless steels and nickel-base alloys (base materials as well as weld metals). The reactor pressure vessel (RPV) or a boiling water reactor (BWR) is made of low alloy steel. The inside surface is combined with stainless steel to avoid corrosion.

Another future perspective of the welding is related to autonomous systems for shipbuilding and offshore industry, which would allow to have faster construction time. Within this context, industrial robots are projected to replace labor efforts in actual manufacturing and can be seen as the technical form of smart shipbuilding. However, most of the conventional welding robots lack in terms of flexibility and many welding operations in shipyards are still made by hand. Analyses of autonomous robotic welding in ship building have been attempted [156–158]. The main drawback is that they need rollers or guide rails that consume much time in terms of installation and time and movements. Separating the intelligent robotic welding (RW) into a number of small tasks could lead to a better result [159]. An alternative way could be the improvement of robots that could recognize the seams to weld. In works by Tsai [160], and Zhang [161] positively identified single weld seams in laboratory conditions. Still the problem could be much more difficult to solve since workpieces in shipyards generally involve complex weld seam configurations.

The current progresses can give the operator the capability to control the system by entering parameters. This means that the operator does not need particular knowledge about robot programming. Depending on the difficulty of the products, the robots can be automated by direct data entry or by importing 3D CAD models. The major advantage of RW is that it can guarantee products with a uniform quality. Figure 25 shows an autonomous welding line robot for shipbuilding. The figure is taken from the website <https://www.kranendonk.com/branches/shipbuilding/> (accessed date 14 May 2022).



**Figure 25.** Autonomous welding line robot for shipbuilding (<https://www.kranendonk.com/branches/shipbuilding/>, accessed date 14 May 2022.)

However, the fatigue behavior of the welded joints, fabricated using RW, was investigated in a few studies, such as [162], where the fatigue responses of SM50A carbon steel T-shaped welded joints, fabricated from robotic and manual welding techniques, were compared.

The fatigue strength of the welded joints depends on the weld quality. The weld quality assurance is required especially for RW in serial production, so a new online method, based on laser scanner technology, could be useful. Stenber et al. [16] proposed the ONLINE system, which is a tool for a rapid evaluation of the weld quality in order to optimize the welding process parameters.

In addition, when dealing with complex and labor-intensive products, one future perspective of the Industry 4.0 revolution related to welding could be its substitution with advancing autonomous technologies such as additive manufacturing (AM) methods [163,164]. Within this context, the wire arc additive manufacturing (WAAM) technique has shown some potential application in shipbuilding and the marine industry for the production of large-scale metal components, particularly for complicated double-curved parts. The use of WAAM technology for the manufacturing of ships parts such as a bulbous bow, ruder and ship propeller, were analyzed and proposed in [163]. Recently, a 3D printed ship's propeller, manufactured with the use of the WAAM technology, known as the "WAAMPeller", was produced in the Netherlands by a group of companies that includes Damen Shipyards Group, RAMLAB, Promarin, Autodesk, and Bureau Veritas, as reported in the website [www.portofrotterdam.com/en/news-and-press-releases/ramlab-develops-first-3d-printed-marine-propeller](http://www.portofrotterdam.com/en/news-and-press-releases/ramlab-develops-first-3d-printed-marine-propeller) (accessed date 14 May 2022).

A functionally graded material (FGM) consisting of carbon–manganese steel and duplex stainless steel, fabricated by WAAM for marine risers, was investigated in [165].

Laminated metal composites (LMCs), consisting of multiple bilayers of alternating layers of ductile and high-strength steel, processed by WAAM using a computer code guided welding robot, were investigated in [166]. The WAAM LMCs, produced by RW, could be applied also in the marine industry.



#### 4. Conclusions

There are several approaches in the fatigue design framework of steel and aluminum alloys welded structures. They are generally classified as nominal, structural, local and fracture mechanics approaches.

The traditional approaches, based on nominal and hot spot stresses, are conservative. The local approaches give more accurate results but require FE models with accurate and fine mesh. Some local approaches, proposed and applied in the technical literature, are based on local quantities, such as stress (NSIF, PSM), strain energy (SED), critical distance (CDM), and temperature (TM).

The fatigue analysis of ship and offshore welded structures is a complex task because their fatigue strength and durability depend on several parameters (local geometrical discontinuity, service loadings, environmental conditions, thickness plate, manufacturing process, residual stresses, defects, and materials properties), so the choice of the fatigue assessment approach depends on the specific application. The review of the different fatigue assessment approaches allows to obtain new insights in order to select the approach that is more suitable for a specific application, aiming to extend the service life of ship and offshore welded structures subjected to fatigue loadings.

A first distinction should be done between the fatigue analysis of the welded joints, such as the ones reported in the current standards, and the large welded structures.

The first issue of this study is the critical analysis of the current codes on the fatigue design of welded structures, which are accepted by some of the major Ship Classification Societies and based on the nominal stress approach. The current codes report the S–N curves of the different fatigue class of the welded joints; this weld classification is based not only on the geometry of the joint but depends also on the dominant loading mode. The codes are based on the assumption that the S–N curves of welded joints with different geometries have about the same slope for a specific material. It was demonstrated that the codes are very conservative, and that the TM can give reliable and fast predictions of the fatigue life and strength of the welded joints, reported in the current codes or others. This approach is able to take into account the weld quality and the presence of defects, unlike the codes.

Moreover, the nominal stresses are not always easy to be evaluated in the real welded structures with complex geometries, so other fatigue approaches are required.

An interesting approach for HCF life predictions is the PSM. Although, the PSM has never been applied to welded joints for shipbuilding and offshore structure, to the authors' knowledge, the 3D modeling of large-scale structures, such as ships and offshore structures, is increasing rapidly, pushing the need for more efficient and time-saving fatigue assessment approaches, thus the 3D PSM could be applied in shipbuilding and offshore structures, as it requires relative coarse meshes in FEA.

Some fatigue cracks have been detected in ship welded structures within a few years of their service life; their fatigue life cannot be adequately predicted by the HCF approaches, but LCF approaches are required. The most suitable approaches for LCF life predictions are the effective notch strain approach, that requires that the elastic–plastic material curves are priorly known, and the equivalent structural strain approach, that presents the same advantages of the equivalent structural stress method and can be applied using linear FE models if controlled displacement tests are performed. In addition, being that the equivalent structural stress/strain approaches are mesh insensitive, could be easily applied for large-scale structures and not only in simple welded ship details or specimens.

If the fatigue cracks have reached a significant length, which can be measured by NDT, the crack initiation phase can be neglected, and the fracture mechanics approaches could be applied for predicting the crack propagation and the fatigue life of the weld.

The fatigue assessment of welded joints becomes more complex when variable amplitude fatigue loadings and multiaxial stress state occur, and the multiaxial fatigue life prediction under VAL remains an open issue. Reliable predictions could be obtained for



these loading conditions, using some fatigue approaches, such as TCD, QTM and energy approaches.

A critical plane approach was applied along with TCD to estimate the multiaxial fatigue life of steel and aluminum welded joints.

The marine and offshore welded structures are generally subjected to VA fatigue loads during their service lives. The current codes suggest the Palmgren–Miner linear damage summation rule for predicting their residual fatigue life, but this rule does not consider the loading sequence effect. Thus, the QTM was developed in order to consider the nonlinear damage accumulation under VAL and the fatigue loading sequence effect for predicting the VAL fatigue life.

The need for using different materials to optimize weight and structural performance of ships and marine structures is rapidly increasing. Within this context, the challenge of joining different materials denotes an essential task, and several dissimilar welding technologies are being performed. The most used type of dissimilar welded joints is nowadays represented by the Al/Steel type. Due to the difficulty of connecting aluminum to steel by means of the traditional welding technique, the most reliable welding technique appears to be explosion welding (EXW). Other properties, such as higher fatigue and static strength enhanced corrosion resistance weight reduction, are needed for offshore and oil and gas structures. The research is continuously progressing in this direction, and some potential solutions to weld light- corrosion-resistant and high strength materials are starting to be individuated.

At last, the use of autonomous welding robots denotes a new frontier in marine welded structures, although important progress should still be made before they can be implemented by most industries.

In conclusion, the welded joints should be designed with an adequate weld quality according to the concept “weld for purpose”.

**Author Contributions:** Conceptualization, V.C. and P.C.; writing—original draft preparation, V.C. and P.C.; writing—review and editing, V.C. and P.C.; visualization, V.C. and P.C.; supervision, V.C. and P.C. All authors have read and agreed to the published version of the manuscript.

**Funding:** This research received no external funding.

**Conflicts of Interest:** The authors declare no conflict of interest.

## References

1. Hirdaris, S.E.; Bai, W.; Dessi, D.; Ergin, A.; Gu, X.; Hermundstad, O.A.; Huijsmans, R.; Iijima, K.; Nielsen, U.D.; Parunov, J.; et al. Loads for Use in the Design of Ships and Offshore Structures. *Ocean Eng.* **2014**, *78*, 131–174. <https://doi.org/10.1016/j.oceaneng.2013.09.012>.
2. Erny, C.; Thevenet, D.; Cognard, J.Y.; Körner, M. Fatigue Life Prediction of Welded Ship Details. *Mar. Struct.* **2012**, *25*, 13–32. <https://doi.org/10.1016/j.marstruc.2011.10.001>.
3. Amirafshari, P.; Barltrop, N.; Wright, M.; Kolios, A. Weld Defect Frequency, Size Statistics and Probabilistic Models for Ship Structures. *Int. J. Fatigue* **2021**, *145*, 106069. <https://doi.org/10.1016/j.ijfatigue.2020.106069>.
4. Tveiten, B.W.; Moan, T. Determination of Structural Stress for Fatigue Assessment of Welded Aluminum Ship Details. *Mar. Struct.* **2000**, *13*, 189–212. [https://doi.org/10.1016/S0951-8339\(00\)00022-8](https://doi.org/10.1016/S0951-8339(00)00022-8).
5. Mei, X.; Xiong, M. Effects of Second-Order Hydrodynamics on the Dynamic Responses and Fatigue Damage of a 15 MW Floating Offshore Wind Turbine. *J. Mar. Sci. Eng.* **2021**, *9*, 1232. <https://doi.org/10.3390/jmse9111232>.
6. Syed Ahmad, S.Z.A.; Abu Husain, M.K.; Mohd Zaki, N.I.; Mukhlas, N.A.; Mat Soom, E.; Azman, N.U.; Najafian, G. Offshore Structural Reliability Assessment by Probabilistic Procedures—A Review. *J. Mar. Sci. Eng.* **2021**, *9*, 998. <https://doi.org/10.3390/jmse9090998>.
7. Jimenez-Martinez, M. Fatigue of Offshore Structures: A Review of Statistical Fatigue Damage Assessment for Stochastic Loadings. *Int. J. Fatigue* **2020**, *132*, 105327. <https://doi.org/10.1016/j.ijfatigue.2019.105327>.
8. Pinheiro, B. de C.; Pasqualino, I.P. Fatigue Analysis of Damaged Steel Pipelines under Cyclic Internal Pressure. *Int. J. Fatigue* **2009**, *31*, 962–973. <https://doi.org/10.1016/j.ijfatigue.2008.09.006>.
9. Yang, Q.; Li, G.; Mu, W.; Liu, G.; Sun, H. Identification of Crack Length and Angle at the Center Weld Seam of Offshore Platforms Using a Neural Network Approach. *J. Mar. Sci. Eng.* **2020**, *8*, 40. <https://doi.org/10.3390/jmse8010040>.
10. Saini, D.S.; Karmakar, D.; Ray-Chaudhuri, S. A Review of Stress Concentration Factors in Tubular and Non-Tubular Joints for Design of Offshore Installations. *J. Ocean Eng. Sci.* **2016**, *1*, 186–202. <https://doi.org/10.1016/j.joes.2016.06.006>.

11. Adedipe, O.; Brennan, F.; Kolios, A. Review of Corrosion Fatigue in Offshore Structures: Present Status and Challenges in the Offshore Wind Sector. *Renew. Sustain. Energy Rev.* **2016**, *61*, 141–154. <https://doi.org/10.1016/j.rser.2016.02.017>.
12. Albiez, M.; Damm, J.; Ummenhofer, T.; Ehard, H.; Schuler, C.; Kaufmann, M.; Vallée, T.; Myslicki, S. Hybrid Joining of Jacket Structures for Offshore Wind Turbines—Validation under Static and Dynamic Loading at Medium and Large Scale. *Eng. Struct.* **2022**, *252*, 112412. <https://doi.org/10.1016/j.engstruct.2021.113595>.
13. Corigliano, P.; Crupi, V.; Fricke, W.; Friedrich, N.; Guglielmino, E. Experimental and Numerical Analysis of Fillet-Welded Joints under Low-Cycle Fatigue Loading by Means of Full-Field Techniques. *Proc. Inst. Mech. Eng. Part C: J. Mech. Eng. Sci.* **2015**, *229*, 1327–1338. <https://doi.org/10.1177/0954406215571462>.
14. Schumacher, A.; Borges, L.C.; Nussbaumer, A. A Critical Examination of the Size Effect Correction for Welded Steel Tubular Joints. *Int. J. Fatigue* **2009**, *31*, 1422–1433. <https://doi.org/10.1016/j.ijfatigue.2009.04.003>.
15. Crupi, V.; Guglielmino, E.; Maestro, M.; Marinò, A. Thinness Effect on the Fatigue Strength of AH36 Steel Plates Used in Shipbuilding. In Proceedings of the NAV 2009, 16th International Conference on Ship and Shipping Research, Messina, Italy, 25 November 2009; pp. 189–197.
16. Stenberg, T.; Barsoum, Z.; Åstrand, E.; Öberg, A. E.; Schneider, C.; Hedegård, J. Quality Control and Assurance in Fabrication of Welded Structures Subjected to Fatigue Loading. *Weld. World* **2017**, *61*, 1003–1015. <https://doi.org/10.1007/s40194-017-0490-5>.
17. Jonsson, B.; Dobmann, G.; Hobbacher, A.F.; Kassner, M.; Marquis, G. *IIW Guidelines on Weld Quality in Relationship to Fatigue Strength*; Springer International Publishing: Cham, Switzerland, 2016; ISBN 978-3-319-19197-3.
18. Amirafshari, P.; Barltrop, N.; Bharadwaj, U.; Wright, M.; Oterkus, S. A Review of Nondestructive Examination Methods for New-Building Ships Undergoing Classification Society Survey. *J. Ship Prod. Des.* **2017**, *34*, 9–19. <https://doi.org/10.5957/JSPD.33.2.160039>.
19. Madi, Y.; Matheron, P.; Recho, N.; Mongabure, P. Low Cycle Fatigue of Welded Joints: New Experimental Approach. *Nucl. Eng. Des.* **2004**, *228*, 161–177. <https://doi.org/10.1016/j.nucengdes.2003.06.016>.
20. Yan, X.; Huang, X.; Huang, Y.; Cui, W. Prediction of Fatigue Crack Growth in a Ship Detail under Wave-Induced Loading. *Ocean Eng.* **2016**, *113*, 246–254. <https://doi.org/10.1016/j.oceaneng.2015.10.056>.
21. Böhm, M.; Kowalski, M. Fatigue Life Estimation of Explosive Cladded Transition Joints with the Use of the Spectral Method for the Case of a Random Sea State. *Mar. Struct.* **2020**, *71*, 102739. <https://doi.org/10.1016/j.marstruct.2020.102739>.
22. Osawa, N.; De Gracia, L.; Iijima, K.; Yamamoto, N.; Matsumoto, K. Study on Fatigue Strength of Welded Joints Subject to Intermittently Whipping Superimposed Wave Load. In *Lecture Notes in Civil Engineering*; Springer: Singapore, 2021; Volume 64, pp. 454–472. ISBN 9789811546716.
23. Woloszyk, K.; Garbatov, Y.; Kłosowski, P. Stress–Strain Model of Lower Corroded Steel Plates of Normal Strength for Fitness-for-Purpose Analyses. *Constr. Build. Mater.* **2022**, *323*, 126560. <https://doi.org/10.1016/j.conbuildmat.2022.126560>.
24. Garbatov, Y.; Guedes Soares, C.; Parunov, J. Fatigue Strength Experiments of Corroded Small Scale Steel Specimens. *Int. J. Fatigue* **2014**, *59*, 137–144. <https://doi.org/10.1016/j.ijfatigue.2013.09.005>.
25. Braun, M.; Ehlers, S. Review of Methods for the High-Cycle Fatigue Strength Assessment of Steel Structures Subjected to Sub-Zero Temperature. *Mar. Struct.* **2022**, *82*, 103153. <https://doi.org/10.1016/j.marstruct.2021.103153>.
26. Hobbacher, A. *Fatigue Design of Welded Joints and Components*; Woodhead Publishing: Sawston, UK, 1996; ISBN 1855733153.
27. Hobbacher, A. *Recommendations for fatigue design of welded joints and components*; IIW document IIW-1823-07 ex XIII-2151r4-07/XV-1254r4-07; doc. XIII-2151r4-07/XV-1254r4-07; International Institute of Welding: Paris, France, 2008.
28. EN 1993-1-9. Eurocode 3: Design of Steel Structures—Part 1–9: Fatigue; CEN: Brussels, Belgium, 2005.
29. EN 1999-1-3. Eurocode 9: Design of Aluminium Structures—Part 1–3: Structures Susceptible to Fatigue; CEN: Brussels, Belgium, 2011.
30. Crupi, V.; Guglielmino, E.; Maestro, M.; Marinò, A. Fatigue Analysis of Butt Welded AH36 Steel Joints: Thermographic Method and Design S-N Curve. *Mar. Struct.* **2009**, *22*, 373–386. <https://doi.org/10.1016/j.marstruct.2009.03.001>.
31. Fricke, W.; Cui, W.; Kierkegaard, H.; Kihl, D.; Koval, M.; Mikkola, T.; Parmentier, G.; Toyosada, M.; Yoon, J.H. Comparative Fatigue Strength Assessment of a Structural Detail in a Containership Using Various Approaches of Classification Societies. *Mar. Struct.* **2002**, *15*, 1–13. [https://doi.org/10.1016/S0951-8339\(01\)00016-8](https://doi.org/10.1016/S0951-8339(01)00016-8).
32. Fricke, W. Recent Developments and Future Challenges in Fatigue Strength Assessment of Welded Joints. *Proc. Inst. Mech. Eng. Part C: J. Mech. Eng. Sci.* **2015**, *229*, 1224–1239. <https://doi.org/10.1177/0954406214550015>.
33. Radaj, D.; Sonsino, C.M.; Fricke, W. Recent Developments in Local Concepts of Fatigue Assessment of Welded Joints. *Int. J. Fatigue* **2009**, *31*, 2–11. <https://doi.org/10.1016/j.ijfatigue.2008.05.019>.
34. Dong, P.; Pei, X.; Xing, S.; Kim, M.H. A Structural Strain Method for Low-Cycle Fatigue Evaluation of Welded Components. *Int. J. Press. Vessel. Pip.* **2014**, *119*, 39–51. <https://doi.org/10.1016/j.ijpvp.2014.03.003>.
35. Pei, X.; Dong, P. An Analytically Formulated Structural Strain Method for Fatigue Evaluation of Welded Components Incorporating Nonlinear Hardening Effects. *Fatigue Fract. Eng. Mater. Struct.* **2019**, *42*, 239–255. <https://doi.org/10.1111/ffe.12900>.
36. Han, Q.; Wang, P.; Lu, Y. Path-dependent Multiaxial Fatigue Prediction of Welded Joints Using Structural Strain Method. *Fatigue Fract. Eng. Mater. Struct.* **2021**, *44*, 2800–2826. <https://doi.org/10.1111/ffe.13550>.
37. Lazzarin, P.; Tovo, R. A Notch Intensity Factor Approach to the Stress Analysis of Welds. *Fatigue Fract. Eng. Mater. Struct.* **1998**, *21*, 1089–1103. <https://doi.org/10.1046/j.1460-2695.1998.00097.x>.
38. Atzori, B.; Lazzarin, P.; Meneghetti, G.; Ricotta, M. Fatigue Design of Complex Welded Structures. *Int. J. Fatigue* **2009**, *31*, 59–69. <https://doi.org/10.1016/j.ijfatigue.2008.02.013>.

39. Saiprasertkit, K. Fatigue Strength Assessment of Load-Carrying Cruciform Joints in Low- and High-Cycle Fatigue Region Based on Effective Notch Strain Concept. *Weld. World* **2014**, *58*, 455–467. <https://doi.org/10.1007/s40194-014-0129-8>.
40. Saiprasertkit, K.; Hanji, T.; Miki, C. Local Strain Estimation Method for Low- and High-Cycle Fatigue Strength Evaluation. *Int. J. Fatigue* **2012**, *40*, 1–6. <https://doi.org/10.1016/j.ijfatigue.2012.01.021>.
41. Meneghetti, G.; Lazzarin, P. Significance of the Elastic Peak Stress Evaluated by FE Analyses at the Point of Singularity of Sharp V-Notched Components. *Fatigue Fract. Eng. Mater. Struct.* **2007**, *30*, 95–106. <https://doi.org/10.1111/j.1460-2695.2006.01084.x>.
42. Meneghetti, G.; Guzzella, C. The Peak Stress Method to Estimate the Mode I Notch Stress Intensity Factor in Welded Joints Using Three-Dimensional Finite Element Models. *Eng. Fract. Mech.* **2014**, *115*, 154–171. <https://doi.org/10.1016/j.engfracmech.2013.11.002>.
43. Chapetti, M.D.; Jaureguizar, L.F. Fatigue Behavior Prediction of Welded Joints by Using an Integrated Fracture Mechanics Approach. *Int. J. Fatigue* **2012**, *43*, 43–53. <https://doi.org/10.1016/j.ijfatigue.2012.02.004>.
44. Zerbst, U.; Madaia, M. Fracture Mechanics Based Assessment of the Fatigue Strength: Approach for the Determination of the Initial Crack Size. *Fatigue Fract. Eng. Mater. Struct.* **2015**, *38*, 1066–1075. <https://doi.org/10.1111/ffe.12288>.
45. Lazzarin, P.; Zambardi, R. A Finite-Volume-Energy Based Approach to Predict the Static and Fatigue Behavior of Components with Sharp V-Shaped Notches. *Int. J. Fract.* **2001**, *112*, 275–298. <https://doi.org/10.1023/A:1013595930617>.
46. Livieri, P.; Lazzarin, P. Fatigue Strength of Steel and Aluminium Welded Joints Based on Generalised Stress Intensity Factors and Local Strain Energy Values. *Int. J. Fract.* **2005**, *133*, 247–276. <https://doi.org/10.1007/s10704-005-4043-3>.
47. Taylor, D.; Barrett, N.; Lucano, G. Some New Methods for Predicting Fatigue in Welded Joints. *Int. J. Fatigue* **2002**, *24*, 509–518. [https://doi.org/10.1016/S0142-1123\(01\)00174-8](https://doi.org/10.1016/S0142-1123(01)00174-8).
48. Taylor, D. *The Theory of Critical Distances: A New Perspective in Fracture Mechanics*; Elsevier: Amsterdam, The Netherlands, 2007; ISBN 9780080554723.
49. Crupi, G.; Crupi, V.; Guglielmino, E.; Taylor, D. Fatigue Assessment of Welded Joints Using Critical Distance and Other Methods. *Eng. Fail. Anal.* **2005**, *12*, 129–142. <https://doi.org/10.1016/j.engfailanal.2004.03.005>.
50. Crupi, V.; Guglielmino, E.; Risitano, A.; Taylor, D. Different Methods for Fatigue Assessment of T Welded Joints Used in Ship Structures. *J. Ship Res.* **2007**, *51*, 150–159.
51. Fan, J.L.; Guo, X.L.; Wu, C.W.; Zhao, Y.G. Research on Fatigue Behavior Evaluation and Fatigue Fracture Mechanisms of Cruciform Welded Joints. *Mater. Sci. Eng. A* **2011**, *528*, 8417–8427. <https://doi.org/10.1016/j.msea.2011.08.037>.
52. Williams, P.; Liakat, M.; Khonsari, M.M.; Kabir, O.M. A Thermographic Method for Remaining Fatigue Life Prediction of Welded Joints. *Mater. Des.* **2013**, *51*, 916–923. <https://doi.org/10.1016/j.matdes.2013.04.094>.
53. Wang, X.G.; Crupi, V.; Jiang, C.; Guglielmino, E. Quantitative Thermographic Methodology for Fatigue Life Assessment in a Multiscale Energy Dissipation Framework. *Int. J. Fatigue* **2015**, *81*, 249–256. <https://doi.org/10.1016/j.ijfatigue.2015.08.015>.
54. Wei, W.; Li, C.; Sun, Y.; Xu, H.; Yang, X. Investigation of the Self-Heating of Q460 Butt Joints and an S-N Curve Modeling Method Based on Infrared Thermographic Data for High-Cycle Fatigue. *Metals* **2021**, *11*, 232. <https://doi.org/10.3390/met11020232>.
55. Palumbo, D.; Galietti, U. Characterisation of Steel Welded Joints by Infrared Thermographic Methods. *Quant. InfraRed Thermogr. J.* **2014**, *11*, 29–42. <https://doi.org/10.1080/17686733.2013.874220>.
56. Al Zamzami, I.; Davison, B.; Susmel, L. Nominal and Local Stress Quantities to Design Aluminium-to-Steel Thin Welded Joints against Fatigue. *Int. J. Fatigue* **2019**, *123*, 279–295. <https://doi.org/10.1016/j.ijfatigue.2019.02.018>.
57. Al Zamzami, I.; Di Cocco, V.; Davison, J.B.; Iacoviello, F.; Susmel, L. Static Strength and Design of Aluminium-to-Steel Thin Welded Joints. *Weld. World* **2018**, *62*, 1255–1272. <https://doi.org/10.1007/s40194-018-0634-2>.
58. Shen, W.; Yan, R.; He, F.; Wang, S. Multiaxial Fatigue Analysis of Complex Welded Joints in Notch Stress Approach. *Eng. Fract. Mech.* **2018**, *204*, 344–360. <https://doi.org/10.1016/j.engfracmech.2018.10.035>.
59. Sonsino, C.M.; Radaj, D.; Brandt, U.; Lehrke, H.P. Fatigue Assessment of Welded Joints in AlMg 4.5Mn Aluminum Alloy (AA 5083) by Local Approaches. *Int. J. Fatigue* **1999**, *21*, 985–999. [https://doi.org/10.1016/S0142-1123\(99\)00049-3](https://doi.org/10.1016/S0142-1123(99)00049-3).
60. Multiaxial Notch Fatigue. *Aircr. Eng. Aerosp. Technol.* **2009**, *81*, 24–31. <https://doi.org/10.1108/aeat.2009.12781dae.001>.
61. Al Zamzami, I.; Susmel, L. On the Use of Hot-Spot Stresses, Effective Notch Stresses and the Point Method to Estimate Lifetime of Inclined Welds Subjected to Uniaxial Fatigue Loading. *Int. J. Fatigue* **2018**, *117*, 432–449. <https://doi.org/10.1016/j.ijfatigue.2018.08.032>.
62. Wang, P.; Pei, X.; Dong, P.; Song, S. Traction Structural Stress Analysis of Fatigue Behaviors of Rib-to-Deck Joints in Orthotropic Bridge Deck. *Int. J. Fatigue* **2019**, *125*, 11–22. <https://doi.org/10.1016/j.ijfatigue.2019.03.038>.
63. Dong, P. A Structural Stress Definition and Numerical Implementation for Fatigue Analysis of Welded Joints. *Int. J. Fatigue* **2001**, *23*, 865–876. [https://doi.org/10.1016/S0142-1123\(01\)00055-X](https://doi.org/10.1016/S0142-1123(01)00055-X).
64. Pei, X.; Dong, P.; Kim, M.H. A Simplified Structural Strain Method for Low-Cycle Fatigue Evaluation of Girth-Welded Pipe Components. *Int. J. Fatigue* **2020**, *139*, 105732. <https://doi.org/10.1016/j.ijfatigue.2020.105732>.
65. Pei, X.; Dong, P.; Xing, S. A Structural Strain Parameter for a Unified Treatment of Fatigue Behaviors of Welded Components. *Int. J. Fatigue* **2019**, *124*, 444–460. <https://doi.org/10.1016/j.ijfatigue.2019.03.010>.
66. Fischer, C.; Fricke, W.; Rizzo, C.M. Review of the Fatigue Strength of Welded Joints Based on the Notch Stress Intensity Factor and SED Approaches. *Int. J. Fatigue* **2016**, *84*, 59–66. <https://doi.org/10.1016/j.ijfatigue.2015.11.015>.
67. Meneghetti, G.; Campagnolo, A. State-of-the-Art Review of Peak Stress Method for Fatigue Strength Assessment of Welded Joints. *Int. J. Fatigue* **2020**, *139*, 105705. <https://doi.org/10.1016/j.ijfatigue.2020.105705>.

68. Song, W.; Liu, X. High Cycle Fatigue Assessment of Steel Load-Carrying Cruciform Welded Joints: An Overview of Recent Results. *Frat. Ed Integrita Strutt.* **2018**, *12*, 94–101. <https://doi.org/10.3221/IGF-ESIS.46.10>.
69. Meneghetti, G.; Campagnolo, A.; Avalle, M.; Castagnetti, D.; Colussi, M.; Corigliano, P.; De Agostinis, M.; Dragoni, E.; Fontanari, V.; Frendo, F.; et al. Rapid Evaluation of Notch Stress Intensity Factors Using the Peak Stress Method: Comparison of Commercial Finite Element Codes for a Range of Mesh Patterns. *Fatigue Fract. Eng. Mater. Struct.* **2018**, *41*, 1044–1063. <https://doi.org/10.1111/ffe.12751>.
70. Dong, Y.; Garbatov, Y.; Guedes Soares, C. Improved Effective Notch Strain Approach for Fatigue Reliability Assessment of Load-Carrying Fillet Welded Cruciform Joints in Low and High Cycle Fatigue. *Mar. Struct.* **2021**, *75*, 102849. <https://doi.org/10.1016/j.marstruc.2020.102849>.
71. Polezhayeva, H.; Toupis, A.I.; Galloway, A.M.; Molter, L.; Ahmad, B.; Fitzpatrick, M.E. Fatigue Performance of Friction Stir Welded Marine Grade Steel. *Int. J. Fatigue* **2015**, *81*, 162–170. <https://doi.org/10.1016/j.ijfatigue.2015.08.003>.
72. Van Lieshout, P.S.; Den Besten, J.H.; Kaminski, M.L. Comparative Study of Multiaxial Fatigue Methods Applied to Welded Joints in Marine Structures. *Frat. Ed Integrita Strutt.* **2016**, *10*, 173–192. <https://doi.org/10.3221/IGF-ESIS.37.24>.
73. Hobbacher, A.F. The New IIW Recommendations for Fatigue Assessment of Welded Joints and Components—A Comprehensive Code Recently Updated. *Int. J. Fatigue* **2009**, *31*, 50–58. <https://doi.org/10.1016/j.ijfatigue.2008.04.002>.
74. Xiao, Z.G.; Yamada, K. A Method of Determining Geometric Stress for Fatigue Strength Evaluation of Steel Welded Joints. *Int. J. Fatigue* **2004**, *26*, 1277–1293. <https://doi.org/10.1016/j.ijfatigue.2004.05.001>.
75. Kim, Y.; Oh, J.S.; Jeon, S.H. Novel Hot Spot Stress Calculations for Welded Joints Using 3D Solid Finite Elements. *Mar. Struct.* **2015**, *44*, 1–18. <https://doi.org/10.1016/j.marstruc.2015.07.004>.
76. Maddox, S.J. Review of Fatigue Assessment Procedures for Welded Aluminium Structures. *Int. J. Fatigue* **2003**, *25*, 1359–1378. [https://doi.org/10.1016/S0142-1123\(03\)00063-X](https://doi.org/10.1016/S0142-1123(03)00063-X).
77. Fricke, W. Recommended Hot-Spot Analysis Procedure for Structural Details of Ships and FPSOs Based on Round-Robin FE Analyses. *Int. J. Offshore Polar Eng.* **2002**, *12*.
78. Lee, J.H.; Dong, P.; Kim, M.H. Low-Cycle Fatigue Evaluation for Girth-Welded Pipes Based on the Structural Strain Method Considering Cyclic Material Behavior. *Int. J. Nav. Archit. Ocean Eng.* **2020**, *12*, 868–880. <https://doi.org/10.1016/j.ijnaoe.2020.08.005>.
79. Yang, H.; Wang, P.; Qian, H.; Dong, P. Fatigue Performance of Different Rib-to-Deck Connections Using Traction Structural Stress Method. *Appl. Sci.* **2020**, *10*, 1239. <https://doi.org/10.3390/app10041239>.
80. Kozy, B. *Manual for Design, Construction, and Maintenance of Orthotropic Steel Bridges*; FHWA: Washington, DC, USA, 2012.
81. Ravi, S.K.; Dong, P. A Spectral Fatigue Method Incorporating Non-Proportional Multiaxial Loading. *Int. J. Fatigue* **2020**, *131*, 105300. <https://doi.org/10.1016/j.ijfatigue.2019.105300>.
82. Xing, S.; Dong, P.; Threstha, A. Analysis of Fatigue Failure Mode Transition in Load-Carrying Fillet-Welded Connections. *Mar. Struct.* **2016**, *46*, 102–126. <https://doi.org/10.1016/j.marstruc.2016.01.001>.
83. Dong, P.; American Society of Mechanical Engineers. *The Master S-N Curve Method : An Implementation for Fatigue Evaluation of Welded Components in the ASME B & PV Code, Section VIII, Division 2 and API 579-1/ASME FFS-1*; Welding Research Council: New York, NY, USA, 2010; ISBN 9781581455304.
84. Corigliano, P.; Crupi, V.; Pei, X.; Dong, P. DIC-Based Structural Strain Approach for Low-Cycle Fatigue Assessment of AA 5083 Welded Joints. *Theor. Appl. Fract. Mech.* **2021**, *116*, 103090. <https://doi.org/10.1016/j.tafmec.2021.103090>.
85. Corigliano, P. On the Compression Instability during Static and Low-Cycle Fatigue Loadings of AA 5083 Welded Joints: Full-Field and Numerical Analyses. *J. Mar. Sci. Eng.* **2022**, *10*, 212. <https://doi.org/10.3390/JMSE10020212>.
86. Fricke, W. Fatigue and Fracture of Ship Structures. In *Encyclopedia of Maritime and Offshore Engineering*; John Wiley & Sons, Ltd.: Chichester, UK, 2017; pp. 1–12.
87. Radaj, D.; Sonsino, C.M.; Fricke, W. *Fatigue Assessment of Welded Joints by Local Approaches: Second Edition*; Elsevier: Amsterdam, The Netherlands, 2006; ISBN 9781855739482.
88. Fricke, W. *IIW Recommendations for the Fatigue Assessment of Welded Structures By Notch Stress Analysis: IIW-2006-09*; Woodhead Publishing: Sawston, UK, 2012; ISBN 9780857098559.
89. Schijve, J. Fatigue Predictions of Welded Joints and the Effective Notch Stress Concept. *Int. J. Fatigue* **2012**, *45*, 31–38. <https://doi.org/10.1016/j.ijfatigue.2012.06.016>.
90. Fricke, W.; Kahl, A. Local Stress Analysis and Fatigue Assessment of Bracket Toes Based on Measured Weld Profile. *Int. Inst. Weld.* **2007**.
91. Tran Nguyen, K.; Garbatov, Y.; Guedes Soares, C. Fatigue Damage Assessment of Corroded Oil Tanker Details Based on Global and Local Stress Approaches. *Int. J. Fatigue* **2012**, *43*, 197–206. <https://doi.org/10.1016/j.ijfatigue.2012.04.004>.
92. Sonsino, C.M. Multiaxial Fatigue Assessment of Welded Joints—Recommendations for Design Codes. *Int. J. Fatigue* **2009**, *31*, 173–187. <https://doi.org/10.1016/j.ijfatigue.2008.06.001>.
93. Nie, J.; Kitazume, D.; Ono, K.; Miyashita, T.; Anami, K.; Matsumura, T. Mechanical Properties and Charpy Absorbed Energy of SBHS400 2019. In Proceedings of the 29th International Ocean and Polar Engineering Conference, Honolulu, Hawaii, USA, 16–21 June 2019.
94. Saiprasertkit, K.; Sasaki, E.; Miki, C. Fatigue Crack Initiation Point of Load Carrying Cruciform Joints in Low and High Cycle Fatigue Regions. *Int. J. Fatigue* **2014**, *59*, 153–158. <https://doi.org/10.1016/j.ijfatigue.2013.09.002>.

95. Fricke, W.; Friedrich, N.; Musumeci, L.; Paetzold, H. Low-Cycle Fatigue Analysis of a Web Frame Corner in Ship Structures. *Weld. World* **2014**, *58*, 319–327. <https://doi.org/10.1007/s40194-014-0117-z>.
96. Dong, Y.; Garbatov, Y.; Guedes Soares, C. Strain-Based Fatigue Reliability Assessment of Welded Joints in Ship Structures. *Mar. Struct.* **2021**, *75*, 102878. <https://doi.org/10.1016/j.marstruc.2020.102878>.
97. Radaj, D. State-of-the-Art Review on Extended Stress Intensity Factor Concepts. *Fatigue Fract. Eng. Mater. Struct.* **2014**, *37*, 1–28. <https://doi.org/10.1111/ffe.12120>.
98. Han, J.W.; Han, S.H.; Shin, B.C.; Kim, J.H. Fatigue Crack Initiation and Propagation Life of Welded Joints. *Key Eng. Mater.* **2005**, 297–300, 781–787. <https://doi.org/10.4028/www.scientific.net/kem.297-300.781>.
99. Glen, L.F.; Dinovitzer, Malik, L.; Basu, R.; Yee, R. *Guide to Damage Tolerance Analysis of Marine Structures*. SSC Report 409; Ship Structure Committee: Washington, DC, USA, 2000.
100. Qi, T.; Huang, X.; Li, L. Spectral-Based Fatigue Crack Propagation Prediction for Very Large Floating Structures. *Mar. Struct.* **2018**, *57*, 193–206. <https://doi.org/10.1016/j.marstruc.2017.10.003>.
101. Mai, Q.A.; Weijtjens, W.; Devriendt, C.; Morato, P.G.; Rigo, P.; Sørensen, J.D. Prediction of Remaining Fatigue Life of Welded Joints in Wind Turbine Support Structures Considering Strain Measurement and a Joint Distribution of Oceanographic Data. *Mar. Struct.* **2019**, *66*, 307–322. <https://doi.org/10.1016/J.MARSTRUC.2019.05.002>.
102. Meneghetti, G. The Peak Stress Method for Fatigue Strength Assessment of Tube-to-Flange Welded Joints under Torsion Loading. *Weld. World* **2013**, *57*, 265–275. <https://doi.org/10.1007/s40194-013-0022-x>.
103. Gandhi, P.; Ramachandra Murthy, D.S.; Raghava, G.; Madhava Rao, A.G. Fatigue Crack Growth in Stiffened Steel Tubular Joints in Seawater Environment. *Eng. Struct.* **2000**, *22*, 1390–1401. [https://doi.org/10.1016/S0141-0296\(99\)00080-2](https://doi.org/10.1016/S0141-0296(99)00080-2).
104. Sonsino, C.M. Comparison of Different Local Design Concepts for the Structural Durability Assessment of Welded Offshore K-Nodes. *Int. J. Fatigue* **2012**, *34*, 27–34. <https://doi.org/10.1016/j.ijfatigue.2010.09.005>.
105. Maljaars, J.; Pijpers, R.; Slot, H. Load Sequence Effects in Fatigue Crack Growth of Thick-Walled Welded C-Mn Steel Members. *Int. J. Fatigue* **2015**, *79*, 10–24. <https://doi.org/10.1016/j.ijfatigue.2015.04.021>.
106. Agerskov, H. Fatigue in Steel Structures under Random Loading. *J. Constr. Steel Res.* **2000**, *53*, 283–305. [https://doi.org/10.1016/S0143-974X\(99\)00042-5](https://doi.org/10.1016/S0143-974X(99)00042-5).
107. Glinka, G. Calculation of Inelastic Notch-Tip Strain-Stress Histories under Cyclic Loading. *Eng. Fract. Mech.* **1985**, *22*, 839–854. [https://doi.org/10.1016/0013-7944\(85\)90112-2](https://doi.org/10.1016/0013-7944(85)90112-2).
108. Dong, Y.; Soares, C.G. Estimation of Effective Notch Strain for Fatigue Strength Assessment of Welded Structures under Multiaxial Stress State. In *Towards Green Marine Technology and Transport*; CRC Press: Boca Raton, FL, USA, 2015; pp. 417–426.
109. Hanji, T.; Saiprasertkit, K.; Miki, C. Low-And High-Cycle Fatigue Behavior of Load-Carrying Cruciform Joints with Incomplete Penetration and Strength under-Match. *Int. J. Steel Struct.* **2011**, *11*, 409–425. <https://doi.org/10.1007/s13296-011-4002-y>.
110. MENEGHETTI, G. The Peak Stress Method Applied to Fatigue Assessments of Steel and Aluminium Fillet-Welded Joints Subjected to Mode I Loading. *Fatigue Fract. Eng. Mater. Struct.* **2008**, *31*, 346–369. <https://doi.org/10.1111/j.1460-2695.2008.01230.x>.
111. Lazzarin, P.; Livieri, P. Notch Stress Intensity Factors and Fatigue Strength of Aluminum and Steel Welded Joints. *Int. J. Fatigue* **2001**, *23*, 225–232. [https://doi.org/10.1016/S0142-1123\(00\)00086-4](https://doi.org/10.1016/S0142-1123(00)00086-4).
112. Berto, F.; Lazzarin, P. A Review of the Volume-Based Strain Energy Density Approach Applied to V-Notches and Welded Structures. *Theor. Appl. Fract. Mech.* **2009**, *52*, 183–194. <https://doi.org/10.1016/j.tafmec.2009.10.001>.
113. Berto, F.; Lazzarin, P. Recent Developments in Brittle and Quasi-Brittle Failure Assessment of Engineering Materials by Means of Local Approaches. *Mater. Sci. Eng. R Rep.* **2014**, *75*, 1–48.
114. Braun, M.; Fischer, C.; Fricke, W.; Ehlers, S. Extension of the Strain Energy Density Method for Fatigue Assessment of Welded Joints to Sub-zero Temperatures. *Fatigue Fract. Eng. Mater. Struct.* **2020**, *43*, 2867–2882. <https://doi.org/10.1111/ffe.13308>.
115. Susmel, L. The Theory of Critical Distances: A Review of Its Applications in Fatigue. *Eng. Fract. Mech.* **2008**, *75*, 1706–1724. <https://doi.org/10.1016/j.engfracmech.2006.12.004>.
116. Susmel, L. Three Different Ways of Using the Modified Wöhler Curve Method to Perform the Multiaxial Fatigue Assessment of Steel and Aluminium Welded Joints. *Eng. Fail. Anal.* **2009**, *16*, 1074–1089. <https://doi.org/10.1016/J.ENGFAILANAL.2008.05.016>.
117. Feng, E.; Wang, X.; Jiang, C.; Crupi, V. Quantitative Thermographic Method for Fatigue Life Prediction under Variable Amplitude Loading. *Fatigue Fract. Eng. Mater. Struct.* **2022**, *45*, 1199–1212. <https://doi.org/10.1111/ffe.13658>.
118. la Rosa, G.; Risitano, a. Thermographic Methodology for Rapid Determination of the Fatigue Limit of Materials and Mechanical Components. *Int. J. Fatigue* **2000**, *22*, 65–73. [https://doi.org/10.1016/S0142-1123\(99\)00088-2](https://doi.org/10.1016/S0142-1123(99)00088-2).
119. Fargione, G.; Geraci, a.; la Rosa, G.; Risitano, a. Rapid Determination of the Fatigue Curve by the Thermographic Method. *Int. J. Fatigue* **2002**, *24*, 11–19. [https://doi.org/10.1016/S0142-1123\(01\)00107-4](https://doi.org/10.1016/S0142-1123(01)00107-4).
120. Luong, M.P. Fatigue Limit Evaluation of Metals Using an Infrared Thermographic Technique. *Mech. Mater.* **1998**, *28*, 155–163. [https://doi.org/10.1016/S0167-6636\(97\)00047-1](https://doi.org/10.1016/S0167-6636(97)00047-1).
121. Meneghetti, G. Analysis of the Fatigue Strength of a Stainless Steel Based on the Energy Dissipation. *Int. J. Fatigue* **2007**, *29*, 81–94. <https://doi.org/10.1016/j.ijfatigue.2006.02.043>.
122. Curà, F.; Curti, G.; Sesana, R. A New Iteration Method for the Thermographic Determination of Fatigue Limit in Steels. *Int. J. Fatigue* **2005**, *27*, 453–459. <https://doi.org/10.1016/j.ijfatigue.2003.12.009>.
123. De Finis, R.; Palumbo, D.; Ancona, F.; Galietti, U. Fatigue Limit Evaluation of Various Martensitic Stainless Steels with New Robust Thermographic Data Analysis. *Int. J. Fatigue* **2015**, *74*, 88–96. <https://doi.org/10.1016/j.ijfatigue.2014.12.010>.

124. Amiri, M.; Khonsari, M.M. Rapid Determination of Fatigue Failure Based on Temperature Evolution: Fully Reversed Bending Load. *Int. J. Fatigue* **2010**, *32*, 382–389. <https://doi.org/10.1016/j.ijfatigue.2009.07.015>.
125. Wang, X.G.; Crupi, V.; Jiang, C.; Feng, E.S.; Guglielmino, E.; Wang, C.S. Energy-Based Approach for Fatigue Life Prediction of Pure Copper. *Int. J. Fatigue* **2017**, *104*, 243–250. <https://doi.org/10.1016/j.ijfatigue.2017.07.025>.
126. Acosta, R.; Wu, H.; Venkat, R.S.; Weber, F.; Tenkamp, J.; Walther, F.; Starke, P. SteBlife, a New Approach for the Accelerated Generation of Metallic Materials' Fatigue Data. *Metals* **2020**, *10*, 798. <https://doi.org/10.3390/met10060798>.
127. Guo, S.; Liu, X.; Zhang, H.; Yan, Z.; Fang, H. Fatigue Limit Evaluation of AZ31B Magnesium Alloy Based on Temperature Distribution Analysis. *Metals* **2020**, *10*, 1331. <https://doi.org/10.3390/met10101331>.
128. Crupi, V.; Epasto, G.; Guglielmino, E.; Marinò, A. Influence of Weld-Porosity Defects on Fatigue Strength of AH36 Butt Joints Used in Ship Structures. *Metals* **2021**, *11*, 444. <https://doi.org/10.3390/met11030444>.
129. Corigliano, P.; Epasto, G.; Guglielmino, E.; Risitano, G. Fatigue Analysis of Marine Welded Joints by Means of DIC and IR Images during Static and Fatigue Tests. *Eng. Fract. Mech.* **2017**, *183*, 26–38. <https://doi.org/10.1016/j.engfracmech.2017.06.012>.
130. Corigliano, P.; Crupi, V.; Guglielmino, E.; Mariano Sili, A. Full-Field Analysis of AL/FE Explosive Welded Joints for Shipbuilding Applications. *Mar. Struct.* **2018**, *57*, 207–218. <https://doi.org/10.1016/j.marstruc.2017.10.004>.
131. Corigliano, P.; Crupi, V. Fatigue Analysis of Ti6AL4V/INCONEL 625 Dissimilar Welded Joints. *Ocean Eng.* **2021**, *221*, 108582. <https://doi.org/10.1016/j.oceaneng.2021.108582>.
132. Micone, N.; de Waele, W. On the Application of Infrared Thermography and Potential Drop for the Accelerated Determination of an S-N Curve. *Exp. Mech.* **2017**, *57*, 143–153. <https://doi.org/10.1007/s11340-016-0194-6>.
133. Benetti 65-Meter Custom Yacht fb274 Takes Shape. Hull and Superstructure Joined Together | Benetti Yachts. Available online: <https://www.benettiyachts.it/news-events/benetti-65-meter-custom-yacht-fb274-takes-shape-hull-and-superstructure-joined-together/> (accessed on 26 February 2022).
134. 70m Benetti Superyacht FB273 Launched—Luxury Projects. Available online: <https://www.luxury-projects.it/70m-benetti-superyacht-fb273-launched/> (accessed on 26 February 2022).
135. Kuryntsev, S. A Review: Laser Welding of Dissimilar Materials (Al/Fe, Al/Ti, Al/Cu)—Methods and Techniques, Microstructure and Properties. *Materials* **2021**, *15*, 122. <https://doi.org/10.3390/MA15010122>.
136. Fukumoto, S.; Tsubakino, H.; Okita, K.; Aritoshi, M.; Tomita, T. Friction Welding Process of 5052 Aluminium Alloy to 304 Stainless Steel. *Mater. Sci. Technol.* **1999**, *15*, 1080–1086. <https://doi.org/10.1179/026708399101506805>.
137. Ozaki, H.; Kutsuna, M. Laser-Roll Welding of a Dissimilar Metal Joint of Low Carbon Steel to Aluminium Alloy Using 2 KW Fibre Laser. *Weld. Int.* **2009**, *23*, 345–352. <https://doi.org/10.1080/09507110802542718>.
138. Boroński, D.; Skibicki, A.; Maćkowiak, P.; Płaczek, D. Modeling and Analysis of Thin-Walled Al/Steel Explosion Welded Transition Joints for Shipbuilding Applications. *Mar. Struct.* **2020**, *74*, 102843. <https://doi.org/10.1016/j.marstruc.2020.102843>.
139. Findik, F. Recent Developments in Explosive Welding. *Mater. Des.* **2011**, *32*, 1081–1093. <https://doi.org/10.1016/j.matdes.2010.10.017>.
140. Corigliano, P.; Crupi, V.; Guglielmino, E. Non Linear Finite Element Simulation of Explosive Welded Joints of Dissimilar Metals for Shipbuilding Applications. *Ocean Eng.* **2018**, *160*, 346–353. <https://doi.org/10.1016/j.oceaneng.2018.04.070>.
141. Wang, W.; Pei, X. An Analytical Structural Strain Method for Steel Umbilical in Low Cycle Fatigue. *J. Offshore Mech. Arct. Eng.* **2019**, *141*, 011605. <https://doi.org/10.1115/1.4040721>.
142. Garbatov, Y. Risk-Based Corrosion Allowance of Oil Tankers. *Ocean Eng.* **2020**, *213*, 107753. <https://doi.org/10.1016/j.oceaneng.2020.107753>.
143. Wołoszyk, K.; Garbatov, Y. An Enhanced Method in Predicting Tensile Behaviour of Corroded Thick Steel Plate Specimens by Using Random Field Approach. *Ocean Eng.* **2020**, *213*, 107803. <https://doi.org/10.1016/j.oceaneng.2020.107803>.
144. Iannuzzi, M.; Barnoush, A.; Johnsen, R. Materials and Corrosion Trends in Offshore and Subsea Oil and Gas Production. *npj Mater. Degrad.* **2017**, *1*, 1–11. <https://doi.org/10.1038/s41529-017-0003-4>.
145. Chandrasekaran, S.; Jain, A. Materials for Ocean Structures. In *Ocean Structures*; CRC Press: Taylor & Francis Group: Boca Raton, FL, USA, 2016; pp. 129–194.
146. Ninomi, M.; Akiyama, S.; Ikeda, M.; Hagiwara, M.; Maruyama The, K. *Update and Trends in Titanium Alloy Riser Applications and Technology*; Japan Institute of Metals: Sendai, Japan, 2007.
147. Peacock, D. Titanium for Offshore Applications. *Mater. World* **1994**, *4*, 696–698.
148. Gao, X.L.; Liu, J.; Zhang, L.J. Dissimilar Metal Welding of Ti6Al4V and Inconel 718 through Pulsed Laser Welding-Induced Eutectic Reaction Technology. *Int. J. Adv. Manuf. Technol.* **2018**, *96*, 1061–1071. <https://doi.org/10.1007/s00170-018-1633-6>.
149. Milititsky, M.; Gittos, F.M.; Smith, S.E.; Marques, V. *Dissimilar Metals for Sub-Sea Use under Cathodic Protection—TWI*; Texas, U., Ed.; Materials Science & Technology: Houston, TX, USA, 2010.
150. Mendoza, B.I.; Maldonado, Z.C.; Albiter, H.A.; Robles, P.E. Dissimilar Welding of Superduplex Stainless Steel/HSLA Steel for Offshore Applications Joined by GTAW. *Engineering* **2010**, *2*, 520–528. <https://doi.org/10.4236/eng.2010.27069>.
151. Sadeghian, M.; Shamanian, M.; Shafyei, A. Effect of Heat Input on Microstructure and Mechanical Properties of Dissimilar Joints between Super Duplex Stainless Steel and High Strength Low Alloy Steel. *Mater. Des.* **2014**, *60*, 678–684. <https://doi.org/10.1016/j.matdes.2014.03.057>.
152. Souza, R.F.; Ruggieri, C.; Zhang, Z. A Framework for Fracture Assessments of Dissimilar Girth Welds in Offshore Pipelines under Bending. *Eng. Fract. Mech.* **2016**, *163*, 66–88. <https://doi.org/10.1016/j.engfracmech.2016.06.011>.



- 
153. Orr, R.S.; Dotson, C. Offshore Nuclear Power Plants. *Nucl. Eng. Des.* **1973**, *25*, 334–349. [https://doi.org/10.1016/0029-5493\(73\)90030-7](https://doi.org/10.1016/0029-5493(73)90030-7).
  154. Briccetti, A.; Buongiorno, J.; Golay, M.; Todreas, N.E. *Siting of an Offshore Floating Nuclear Power Plant*; Massachusetts Institute of Technology: Cambridge, MA, USA, 2014.
  155. Hänninen, H.; Aaltonen, P.; Brederholm, A.; Ehrnsteñ, U.; Gripenberg, H.; Toivonen, A.; Pitkariñ, J.; Virkkunen, I. *Dissimilar Metal Weld Joints and Their Performance in Nuclear Power Plant and Oil Refinery Conditions*; VTT: Espoo, Finland, **2006**.
  156. Rooks, B. Robot Welding in Shipbuilding. *Ind. Robot* **1997**, *24*, 413–417. <https://doi.org/10.1108/01439919710192527>.
  157. Sanders, D.; Tewkesbury, G.; Ndzi, D.; Gegov, A.; Gremont, B.; Little, A. Improving Automatic Robotic Welding in Shipbuilding through the Introduction of a Corner-Finding Algorithm to Help Recognise Shipbuilding Parts. *J. Mar. Sci. Technol.* **2011**, *17*, 231–238. <https://doi.org/10.1007/S00773-011-0154-X>.
  158. Lee, D.; Ku, N.; Kim, T.W.; Kim, J.; Lee, K.Y.; Son, Y.S. Development and Application of an Intelligent Welding Robot System for Shipbuilding. *Robot. Comput.-Integr. Manuf.* **2011**, *27*, 377–388. <https://doi.org/10.1016/J.RCIM.2010.08.006>.
  159. Muhammad, J.; Altun, H.; Abo-Serie, E. Welding Seam Profiling Techniques Based on Active Vision Sensing for Intelligent Robotic Welding. *Int. J. Adv. Manuf. Technol.* **2016**, *88*, 127–145. <https://doi.org/10.1007/S00170-016-8707-0>.
  160. Tsai, M.J.; Lee, H.W.; Ann, N.J. Machine Vision Based Path Planning for a Robotic Golf Club Head Welding System. *Robot. Comput.-Integr. Manuf.* **2011**, *27*, 843–849. <https://doi.org/10.1016/J.RCIM.2011.01.005>.
  161. Zhang, K.; Yan, M.; Huang, T.; Zheng, J.; Li, Z. 3D Reconstruction of Complex Spatial Weld Seam for Autonomous Welding by Laser Structured Light Scanning. *J. Manuf. Processes* **2019**, *39*, 200–207. <https://doi.org/10.1016/J.JMAPRO.2019.02.010>.
  162. Han, C.; Yang, C.; Kim, H.; Park, S. The Effects of Robot Welding and Manual Welding on the Low- and High-Cycle Fatigue Lives of SM50A Carbon Steel Weld Zones. *Adv. Mech. Eng.* **2019**, *11*, 168781401982826. <https://doi.org/10.1177/1687814019828266>.
  163. Taşdemir, A.; Nohut, S. An Overview of Wire Arc Additive Manufacturing (WAAM) in Shipbuilding Industry. *Ships Offshore Struct.* **2021**, *16*, 797–814. <https://doi.org/10.1080/17445302.2020.1786232>.
  164. Astarita, A.; Compatelli, G.; Corigliano, P.; Epasto, G.; Montevicchi, F.; Scherillo, F.; Venturini, G. Microstructure and Mechanical Properties of Specimens Produced Using the Wire-Arc Additive Manufacturing Process. *Proc. Inst. Mech. Eng. Part C J. Mech. Eng. Sci.* **2021**, *235*, 1788–1798. <https://doi.org/10.1177/0954406219883324>.
  165. Chandrasekaran, S.; Hari, S.; Amirthalingam, M. Wire Arc Additive Manufacturing of Functionally Graded Material for Marine Risers. *Mater. Sci. Eng. A* **2020**, *792*, 139530. <https://doi.org/10.1016/j.msea.2020.139530>.
  166. Spalek, N.; Brunow, J.; Braun, M.; Rutner, M. WAAM-Fabricated Laminated Metal Composites. *Metals* **2021**, *11*, 1948. <https://doi.org/10.3390/met11121948>.